International Journal of Nanomedicine

Dovepress
open access to scientific and medical research

Open Access Full Text Article

REVIEW

Advances on Delivery System of Active Ingredients of Dried Toad Skin and Toad Venom

Dan Zhang, Bingtao Zhai, Jing Sun, Jiangxue Cheng, Xiaofei Zhang, Dongyan Guo

State Key Laboratory of Research & Development of Characteristic Qin Medicine Resources (Cultivation), and Shaanxi Key Laboratory of Chinese Medicine Fundamentals and New Drugs Research, and Shaanxi University of Chinese Medicine, Xi'an, 712046, People's Republic of China

Correspondence: Dongyan Guo, Email 2051080@sntcm.edu.cn

Abstract: Dried toad skin (TS) and toad venom (TV) are the dried skin of the *Bufo bufo gargarizans Cantor* and the *Bufo melanostictus Schneider*, which remove the internal organs and the white secretions of the skin and retroauricular glands. Since 2005, cinobufacini preparations have been approved by the State Food and Drug Administration for use as adjuvant therapies in the treatment of various advanced cancers. Meanwhile, bufalenolides has been identified as the main component of TS/TV, exhibiting antitumor activity, inducing apoptosis of cancer cells and inhibiting cancer cell proliferation or metastasis through a variety of signaling pathways. However, clinical agents frequently face limitations such as inherent toxicity at high concentrations and insufficient tumor targeting. Additionally, the development and utilization of these active ingredients are hindered by poor water solubility, low bioavailability, and rapid clearance from the bloodstream. To address these challenges, the design of a targeted drug delivery system (TDDS) aims to enhance drug bioavailability, improve targeting within the body, increase drug efficacy, and reduce adverse reactions. This article reviews the TDDS for TS/TV, and their active components, including passive, active, and stimuli-responsive TDDS, to provide a reference for advancing their clinical development and use.

Keywords: dried toad skin, toad venom, targeted drug delivery system, passive targeted, active targeted, stimuli-responsive targeted

Introduction

To date, cancer continues to be a leading cause of death.[1] The International Agency for Research on Cancer has estimated nearly 20 million new cancer cases and approximately 10 million cancer-related deaths for 2020. Population-based projections suggest that the annual incidence of new cancer cases will rise to 35 million by 2050, a 77% increase from the 2022 levels.[2] According to the latest projections by the American Cancer Society, the United States is expected to report experience approximately 2 million new cancer cases and 611,720 cancer deaths in 2024.[3] Cancer is a disease caused by the uncontrolled proliferation of transformed cells which have evolved through natural selection.[4] Currently, the three primary modalities for cancer treatment include surgical resection, chemotherapeutic agents, and radiotherapy. However, in clinical practice, tumor recurrence and metastasis significantly affect patient prognosis, highlighting the inherent limitations of traditional treatment methods. For example, surgery can lead to recurrence due to incomplete resection, while radiotherapy is often inadequate for addressing metastasis due to its local and selective action, resulting in suboptimal treatment outcomes. Chemotherapy remains a critical treatment modality, but systemic toxicity and multidrug resistance limit its efficacy and hinder its development.[5–7] Therefore, there is an urgent need to discover new anticancer drugs and innovate novel treatment strategies.

Traditional Chinese Medicine (TCM), a therapeutic approach with a history spanning thousands of years, is characterized by its multi-component, multi-target treatment capabilities in contrast to conventional chemotherapy drugs, offering both direct tumor inhibition and indirect antitumor effects through immune enhancement.[8,9] *Bufo bufo gargarizans Cantor* and *Bufo melanostictus Schneider* of the family Bufonidae are traditional medicinal animals, and dried epidermis and dried secretions of the retroauricular and skin glands are known as toad skin (TS) and toad venom (TV). Both possess significant medicinal value with a long history record in the Compendium of Materia Medica.[10]

Received: 20 March 2024
Accepted: 29 June 2024
Published: 18 July 2024

Currently, the State Food and Drug Administration has approved Cinobufacini injection, Cinobufacini capsules, Cinobufacini tablets, and TV injection for the adjuvant treatment of lung, colon, gastric, and other cancers, improving treatment efficacy and patient quality of life. However, adverse reactions including allergic responses, drug fever, and leukopenia limit the clinical application of these preparations.[11] The chemical composition of TS/TV is complex, consisting of bufadienolides (BFN), indole alkaloids, cyclic peptides, organic acids, and other constituents.[12] Among these, BFN is the main antitumor component, structurally characterized by an α-pyranone ring at position 17 of the C-24 steroid,[13] encompassing bufalin (BU), cinobufotalin (CBF), cinobufagin (CBG), resibufogenin (RBG), arenobufagin (ABG) and gamabufotalin (GBF). Numerous studies have demonstrated that these components primarily inhibit cell proliferation, promote cell apoptosis, inhibit tumor angiogenesis, and regulate immune responses, contributing to their effects in liver, lung, colorectal, and breast cancers, among others.[14,15] Despite their significant antitumor potential, these compounds exhibit drawbacks such as rapid metabolism, high toxicity, poor water solubility, and short half-life.[16] Moreover, the ideal anticancer drug should selectively target cancer cells without harming normal cells.[17] Therefore, achieving an ideal anticancer drug requires enhancing drug targeting and overcoming the aforementioned challenges.

With the advancement of science and technology, improving water solubility, reducing toxicity, increasing stability, prolonging half-life, enhancing targeting, and achieving controlled release of drugs in targeted drug delivery system (TDDS) have become a feasible strategy to address these challenges.[18] Consequently, TDDS have emerged as a crucial tool in the process of turning the antitumor active ingredients of TCM into desirable anticancer drugs. Specifically, the use of nanocarriers for the delivery of TS/TV and their active ingredients can effectively improve poor water solubility and enhance drug accumulation at tumor sites through enhanced tumor permeability and retention (EPR) effect, thus reducing toxic side effects to major organs.[19] Moreover, surface modification of nanocarriers with ligands or antibodies enables precise active targeting through specific binding to receptors overexpressed on tumor cells, resulting in improved therapeutic efficacy.[20] Furthermore, biomimetic membrane-based drug delivery systems have gained significant attention due to their superior biocompatibility, immune evasion, and homologous targeting capabilities.[21] At the same time, the tumor microenvironment (TME) and certain nanocarriers facilitate drug targeting through endogenous factors or exogenous responses triggered by physical or chemical stimuli, making drug delivery more controlled and accurate.[22,23] Increasingly, researchers are combining TDDS with TS/TV to address issues like poor solubility, short systemic circulation, significant side effects, and inadequate targeting, providing new insights and enhancing therapeutic efficacy, thereby opening new opportunities.

The noteworthy therapeutic effects of TS/TV have garnered significant attention. Jia et al[24] focused on the antitumor mechanism of TV and its active ingredients. Soumoy et al[25] introduced the anti-cancer mechanism, disadvantages and difficulties in clinical use of BU. And Shao et al[26] summarized the pharmacological activity, structure activity relationship and part of the drug delivery of BFN. However, these studies mainly focused on mechanism investigations, single-component analyses or only partial reviews of delivery characteristics, with a comprehensive Introduction to the various TDDS of TS/TV and their active ingredients still lacking. Thus, this paper presents the delivery capabilities and efficacy characteristics of various monomers, including BU, CBF, CBG, RBG, ABG and GBF, under passive, active, and stimuli-responsive TDDS strategies. We also examine the challenges related to different TDDS and propose potential solutions. Additionally, we address the limitations translating these strategies into clinical practice, providing insights for future clinical applications and suggesting reference points for the development of TS/TV and their active ingredients (Figure 1).

Passive Targeted Drug Delivery System

Passive targeting agents refer to drug-loaded particles that selectively accumulate in tumor tissues by leveraging the pathophysiological conditions and anatomical alterations of the TME.[27] The discontinuous arrangement of vascular endothelial cells in tumors and impaired lymphatic drainage at the tumor site enable NPs to penetrate and accumulate in cancer tissues more readily than in normal tissues. This results in increased permeability and long-term retention of NPs.[28] Thus, the EPR effect has long been considered the most effective passive targeting mechanism for NPs in solid tumors.[29] Enhancing the EPR effect has become a major driving force in the design of passive targeting agents. In passive TDDS, biodegradable, safe, biocompatible and non-immunogenic carrier materials ranging from 1 to 100 nm in

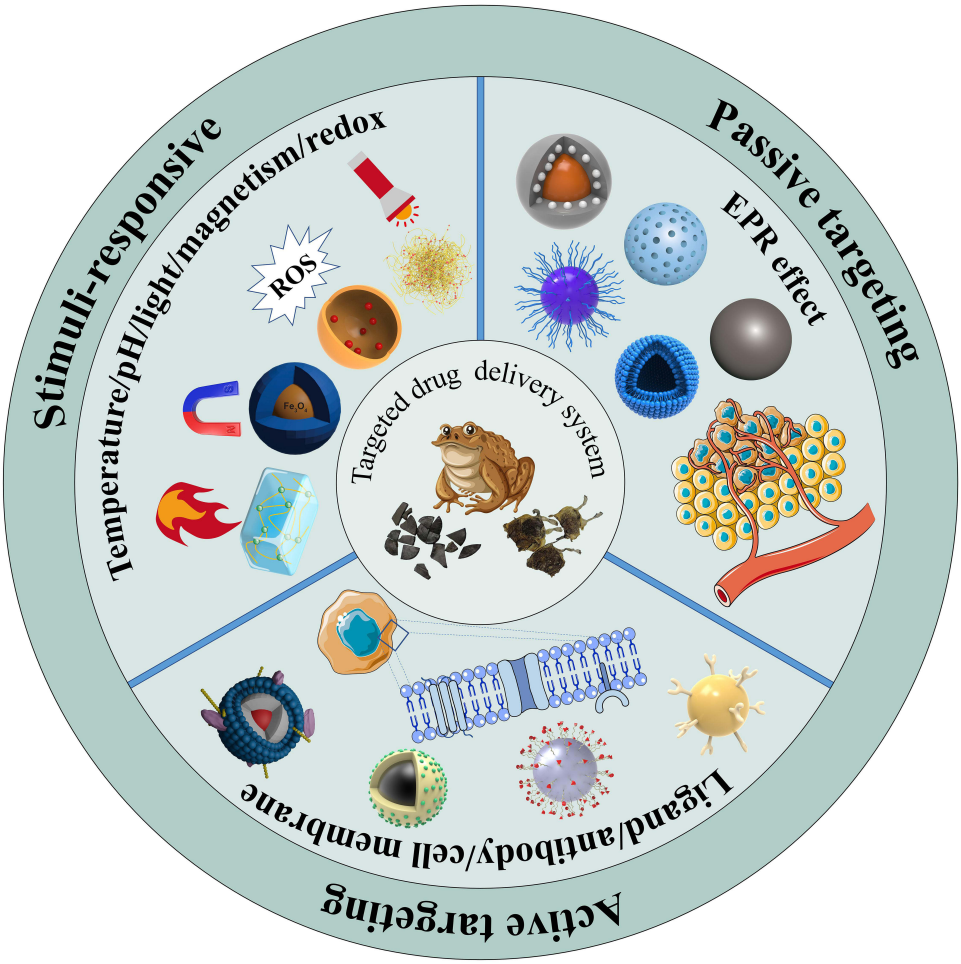

Figure 1 Schematic diagram of targeted drug delivery classification of TS and TV and their active ingredients.

diameter are often used,[30] such as mesoporous silica NPs, solid lipid NPs, liposomes, albumin NPs, polymer NPs, polymer micelles, and so on. The key characteristics of these systems have been summarized in Table 1.

The Mesoporous Silica Nanoparticles

Mesoporous silica NPs (MSNs) are mesostructured bioceramics characterized by an adjustable porous structure and shape, high pore volume, high loading capacity and controlled drug release. MSNs exhibit biodegradability and biocompatibility. Furthermore, the high surface density of silanol groups facilitates functionalization. Therefore, MSNs have become one of the ideal candidates for current TDDS.[61–63] Xiao et al[31] prepared MSNs encapsulating the extractions of TS with a particle size (TSE-MSNs) of (95.63 ± 9.32) nm and a polydispersity index (PDI) of (0.083 ± 0.026). In vitro pharmacodynamic experiments demonstrated that TSE-MSNs induced apoptosis and blocked the cell cycle of HepG2 cells, exerting antitumor effects. In addition, an in vivo tumor inhibition assay in MCF-7 nude mice revealed that TSE-MSNs significantly inhibited tumor growth compared to control group, with no apparent toxic side effects on various organs.

The Polymer Nanoparticles

Polymer NPs are nano-delivery systems composed of natural or synthetic polymers, featuring a matrix of various biodegradable polymers that improve the drug encapsulation efficiency. Additionally, polymer NPs are characterized by straightforward preparation, enhanced drug properties, biocompatibility and biodegradability.[64] Poly (lactic-co-glycolic acid) (PLGA) has been approved by the FDA as an effective carrier for TDDS, noted for its good

Table 1 Passive TDDS of Active Ingredients of TS/TV

Drug Delivery System	Ingredients	Features	Characterization	Pharmacokinetics/Tissue Distribution/ Efficacy	Diseases	Ref., Year
TSE-loaded MSN	Cetyltrimethyl ammonium chloride, tetraethyl orthosilicate, triethanolamine, TSE	1.High EE 2.Good Stability	Mean Size: (95.63±9.32) nm PDI: (0.083±0.026) DL: (14.35±1.89) % specific surface area: 625.31m^2/g	IC_{50} values of HepG2 cell: 0.79 μg/mL; Apoptosis rate of HepG2 cell↑; Tumor growth volume in bearing MCF-7 nude mices↓	Liver cancer	2009[31]
RBG-PLGA/TPGS nanoparticles	RBG, sodium dodecyl sulfate, PLGA-TPGS	1.Good stability 2.Reversal of tumor multidrug resistance	Mean Size: (152.3±2.5) nm PDI: (0.082±0.015) Zeta potential: (−24.1±1.2) mV EE: 79.3% DL: 18.4%:	Cytotoxicity: RBG-P/T NPs>RBG; 5-fluorouracil injection; Cumulative drug release rate in 3 hours: 86.7%; Tumor inhibition rate in bearing HCa-F cell: RBG-P/T NPs>RBG-P NPs>5-fluorouracil injection>Free RBG Pharmacokinetics: AUC, C_{max}↑	Liver cancer	2017[32–36]
BU-loaded PBCA nanoparticles	α-butylcyanoacrylate, BU	Low hemolysis	Mean Size: (151.2±6.1) nm PDI: (0.133±0.024) Zeta potential: (−7.09±0.58) mV EE: (70.812±6.139) % DL: (1.990±0.291) %	Hemolysis rate↓	—	2015[37]
BU-loaded Pluronic-PEI nanoparticles	Pluronic-F127, PEI, BU	Good solubility	Mean Size: 65 nm PDI: 0.214 Zeta potential: (5.87±0.42) mV EE: 75.71% DL: 3.04%	Cellular uptake of HCT116↑; The fluorescence intensity in HCT116: Rhodamine B loaded Pluronic-PEI NPs>Free Rhodamine B; Tumor suppression in bearing HCT116 Balb/c mice: BU loaded Pluronic-PEI NPs>Free BU	Colon cancer	2014[38]
BU-loaded Pluronic-PEI nanoparticles	Pluronic-F127, PEI, BU	Efficient	—	Inhibition and migration rate of LoVo cells overexpressing miR-497: BU loaded Pluronic-PEI NPs>Free BU; In vivo fluorescence imaging: BU loaded Pluronic-PEI NPs>Free BU	Colon cancer	2017[39]
TVE-loaded SLNs	TVE, Glyceryl behenate, poloxamer 188, Soy lecithin	High EE	Mean Size: 71.5 nm, EE: 92.45% DL: 5.26%	Pharmacokinetics: AUC, $T_{1/2}$, C_{max}, MRT↑ Distribution of liver tissue: TVE-SLNs>Free TVE	—	2007[40–43]
TSE-loaded SLNs	Glyceryl behenate, Soy lecithin, TVE, poloxamer 188, TWeen-80	High DL	Mean Size: (138.5±4.2) nm PDI: (0.143±0.023) EE: CBG/RBG: 90.6%/91.51% DL: CBG/RBG: 35.82%/44.15%	Drug release rate↓	—	2016[44,45]

CBG-loaded albumin nanoparticles	BSA, CBG, glutaraldehyde	Efficient	Mean Size: 86.3 nm Zeta potential: −49 mV EE: 79.5% DL: 24.1%	The survival time of the nude mice with orthotopic transplantation ↑; Hepatic damage: Free CBG>Cino-BSA-NP; LD_{50}: Cino-BSA-NP>Free CBG (9.7047>4.1301 mg/kg); Minimum toxicity dosage↑	Liver cancer	2009[46]
BU-loaded albumin nanoparticles	BU, BSA, glutaraldehyde	Biocompatibility	Mean Size: 125.1 nm PDI: 0.140 Zeta potential: −19.24 mV EE: 76.02% DL: 12.62%	Liver and tumor uptake in transplanted liver cancer model mice: Bufalin-BSA-NPs>BU; IC_{50} in SMMS-7721 cell: BU>Bufalin-BSA-NPs; Mean survival time of mice transplanted with hepatocellular carcinoma in situ: Bufalin-BSA-NPs /BU>adriamycin/normal saline Pharmacokinetics: AUC, $t_{1/2.}$, MRT, V↑; C_{max}, CL↓	Liver cancer	2017[47]
BU-loaded PLGA microspheres	PVDF membranes, PLGA, BU	Prolonged effect	Size: (570±60) nm EE: 85.10% DL: 3.84%	The number of administrations ↓; The level of IL-1β, IL-18, IL-6 and TNF-α in CCI model ↓; The duration of analgesia↑	Neuropathic Pain	2022[48]
Toad venom-PLA microspheres	Toad venom, PVA-224, polylactate,	High DL	Size: (1~10) μm DL: (23.4±0.5) % EE: (31.5±1.8) %	Pharmacokinetic: T_{max}, $t_{1/2}$, AUC, MRT↑	Swine enzootic pneumonia	2015[49]
BU-loaded Polymeric micelles	Arginine-terminated lapidated dendrimers, Fmoc-Lys (Mtt)–OH, BU	1.Fast assembling 2.Good aqueous solubility 3.Good biocompatibility	Size: 130 nm Zeta potential: +3.03 mV CMC: 105.38 μmol/L	Cellular uptake and intracellular delivery ↑	—	2019[50]
Toad venom-polymeric micelles	Pluronic-F123, Deoxycholic acid Sodium, Toad venom	High EE	Mean Size: 120 nm EE: 94.12% DL: 0.14%	Gastrointestinal irritation ↑	—	2018[51]
ABG-loaded polymeric nanomicelles	mPEG, PLGA, sodium oleate, ABG	1.Good biocompatibility 2.Whole body delivery	Size: 105 nm PDI: 0.08 EE: 71.9% DL: 4.58%	IC_{50} values in HepG2 cell: pure ABG>ABG-PNs; Cellular uptake of ABG in HepG2: ABG-PNs>the cosolvent group Pharmacokinetics: AUC↑, CL↓	Liver cancer	2017[52]
Bufotenines-loaded liposomes	Soy lecithin-cholesterol (10:3, m/m), Chloroform-methanol (2:1, v/v), bufotenines	Slow release	Mean Size: (130.1±4.06) nm PDI: 0.217 Zeta potential: (−8.00±0.88) mV	Cardiac Specific Markers: CK, LDH↑; The release of bufotenines in 8 h at 37 °C, 100 rpm: Free bufotenines>bufotenines-LPs; In the COX pathway: dhk-PGE1, PGK2,8-iso-PGF2α, 15-keto-PGF1α, 6-keto-PGF1α and PGD3↓; In the LOX metabolic pathway: LTC4, LTB4 and 12-HETrE↓; In the LA metabolic pathway: 9-OxoODE and 13-HODE↓ Pharmacokinetics: AUC, $t_{1/2}$, C_{max}↑; V Cl↓	—	2022[53]

(*Continued*)

https://doi.org/10.2147/IJN.S469742 DovePress

Table 1 (Continued).

Drug Delivery System	Ingredients	Features	Characterization	Pharmacokinetics/Tissue Distribution/ Efficacy	Diseases	Ref., Year
BF211-loaded liposomes	Hspc, DSPE-PEG_{2000}, BF211, Cholesterol	High EE	Size: (164.6±10.3) nm PDI: (0.185±0.017) Zeta potential: (−32.25±2.39) mV EE: (93.24±2.15) %	Blood circulation time↑; Cardiotoxicity↓; Cellular uptake of HepG2↑; Anti-tumor efficiency in mice xenografted with HepG2 cells: BF211@Lipo>Free BF211; Pharmacokinetics: AUC, $t_{1/2}$, C_{max}↑; V, CL↓;	Liver cancer	2021[54]
BU-loaded liposomes	Cholesterol, L-α-phosphatidylchoine, DSPE-PEG_{2000}, BU	Low toxicity	Mean Size: (155.0±8.46) nm Zeta potentials: −18.5 mV EE: (78.40±1.62) %	Cell viabilities of U251↓ Pharmacokinetics: AUC, MRT, $T_{1/2}$↑; $V_{z/F}$ C_{max}↓	—	2017[55]
BU-loaded liposomes	Cholesterol, L-α-phosphatidylchoine, DSPE-PEG_{2000}, BU	Good safety	Mean Size: (155.0±8.46) nm Zeta potentials: (−18.5±4.49) mV EE: (76.31±4.23) %	The sensitivity of cells to BU-PEG-LPs: HCT116>HepG2>U251>A549; The acute toxicity in mice: Free BU>BU-PEG-LPs; Concentration and action time of bufalin in brain↑	—	2019[56]
TVE-loaded liposomes	Cholesterol, lecithin, DSPE-mPEG2000, TVE	Long circulation time	Size: 115 nm Zeta potential: −47.28 mV EE: ~86% DL: 7.3%	Enriched concentration of liver and lung in vivo↑ Pharmacokinetics: AUC, MRT, $T_{1/2}$, C_{max}↑; k, CL↓	—	2020[57]
Bufadienolides-loaded liposomes	Phospholipid PL100, Cholesterol, PEG2000 Bufadienolides	High EE	Mean Size: (86.5±2.7) nm Zeta potential: −15.2 mV EE: BU/CBG/RBG: 94.2%/98.5%/96.4% DL: 1.66%	Pharmacokinetics: AUC, C_{max}, $t_{1/2}$↑; CL↓	—	2022[58]
TSE and BJO co-loaded nanoemulsion	Lecithin, MCT, TSE, BJO	1.Synergistic effect 2.High EE 3.High DL	Size: 155 nm PDI: 0.058 Zeta potential: −35 mV EE: >95% DL: ~15%	IC_{50} and CI values of TES-BJO (2:1) on HepG2 cell: 0.663 (μg/mL) and 0.358; Apoptosis rate of HepG2 cell: TSE-BJO NEs>BJO NES>TSE NEs; The tumor inhibition rate in HepG2 tumor bearing nude mice: TSE-BJO NEs>BJO NES and TSE NEs Pharmacokinetics: AUC, MRT, $T_{1/2}$↑; k, CL↓	Liver cancer	2023[59]
BU-loaded microemulsion	MCT, Triglycerides, A co-surfactant blend of macrogol (15) (Solutol HS 15), Sorbitan monooleate (Span 80), BU	1.High EE 2.Sample Preparation	EE: >90%	Compared with the pure bufalin suspension, the toxicity of the drug-loaded microemulsion was increased by 1.4 times; Apoptosis rate of A549 cell↑ Pharmacokinetics: AUC, $t_{1/2}$, C_{max}, MRT, T_{max}↑	Lung cancer	2018[60]

Abbreviations: EE, encapsulation efficiency; DL, drug load efficiency; PDI, polydispersity index; AUC, area under the curve; MRT, mean residence time; $t_{1/2}$, half-life; C_{max}, maximal concentration; T_{max}, time of maximum concentration, CL, clearance rate; TSE, toad skin extraction; TVE, toad venom extraction; BU, bufalin; CBG, cinobufagin; RBG, resibufogenin; ABG, arenobufagin; BJO, brucea oil; MCT, Medium chain capric/caprylic.

biocompatibility, safety, easy degradation and excellent mechanical properties. It also enhances immunogenicity and improves drug absorption.[65] Xu et al employed PLGA-conjugated vitamin E polyethylene glycol 1000 succinate (TPGS) as a carrier to encapsulate RBG forming RBG-loaded PLGA-TPGS NPs (RBG-P/T NPs) with a particle size of 152.3 nm, and the drug loading efficiency (DL) and encapsulation efficiency (EE) were 18.4% and 79.3%, respectively. The 3 h cumulative drug release rate was 86.7%, and the NPs exhibited good in vitro stability. TPGS facilitates mitochondrial targeting and inhibits P-glycoprotein expression, thereby reversing tumor multidrug resistance. The LD_{50} of RBG-P/T NPs was 2.02 times higher than that of the RBG solution, and the area under the curve (AUC) of RBG in liver was up to three times higher than in plasma and other organ homogenates. In vivo distribution indicated that RBG-P/T NPs prolonged the drug's retention time and increased its concentration in the liver, suggesting potential to mitigate in vivo toxicity, enhance liver targeting, and improve bioavailability. In vitro cellular uptake and toxicity assays demonstrated that RBG-P/T NPs inhibited HepG2 cells, and in the in vivo antitumor assay, the tumor inhibition rate (TIR) of RBG-P/T NPs was 64.93%, significantly surpassing that of the positive control and all other groups.[32–36]

Poly (n-butylcyanoacrylate) (PBCA) is formed by self-polymerization of n-butylcyanoacrylate in an aqueous system with an activator. PBCA NPs can protect drugs from gastric degradation, allowing controlled release in the intestine.[66] Chen et al[37] prepared BU-loaded PBCA NPs (BU-PBCA NPs) by alcohol polymerization. BU-PBCA NPs exhibited uniform in shape, with an average particle size of (51.2 ± 6.1) nm, a PDI of (0.133 ± 0.024), a zeta potential of (−7.09 ± 0.58) mV, an EE of (70.812 ± 6.139) %, and a DL of (1.990 ± 0.291) %. Compared to free BU, BU-PBCA NPs demonstrated lower hemolysis and higher safety.

Pluronic is a hydrophilic polymer that enhances solubility in hydrophobic environments. In addition, Polyetherimide (PEI) improves the stability of its composites. Therefore, Hu et al[38] prepared BU-loaded Pluronic-PEI NPs by the thin film method. The average particle size, PDI and zeta potential were 65 nm, 0.214, (5.87 ± 0.42) mV, and the EE and DL were 75.1% and 3.04%, respectively. In vivo fluorescence imaging experiments showed that BU-loaded Pluronic-PEI NPs had a more potent therapeutic effect on colon cancer than BU alone. The research team further investigated the mechanism of action of the NPs in treating colon cancer. Western blot analysis demonstrated that BU-loaded Pluronic-PEI NPs effectively inhibited the miR-497-mediated IGF1-R-PI3K-Akt signaling pathway. This inhibition leads to downregulation of the pathway, which plays a critical role in promoting tumorigenesis and cancer cell survival. Consequently, this targeted approach results in reduced cell proliferation and increased apoptosis in colon cancer cells, highlighting the therapeutic potential of these NPs in colon cancer treatment.[39]

The Solid Lipid Nanoparticles

Solid lipid NPs (SLNs), ranging in size from 10 to 1000 nm, effectively encapsulate drugs in a solid state at room temperature and facilitate drug release in a liquid state at body temperature. Compared to other traditional carriers, SLNs have the advantages of lower toxicity, longer sustained release of drugs, better cellular uptake, and improved drug bioavailability.[67,68] Yang et al first prepared TV extractions SLNs (TVE-SLNs) by cold-homogenization method, achieving a high EE of 92.45% and a stable preparation process. To address the physicochemical stability problem of SLNs aqueous dispersion, a freeze-dried TVE-SLNs agent was developed to prevent drug degradation and NPs aggregation. In vivo pharmacokinetic studies showed that the freeze-dried agent could delay drug release and mitigate the adverse effects of TVE on blood vessels. Distribution experiments in mice revealed that the lyophilized formulation had better liver targeting compared to aqueous solution.[40–43] There were also studies using SLNs to load toad skin extract (TSE-SLNs) to improve drug solubility and stability. In vitro cumulative release experiments indicated that TSE-SLNs had a certain sustained release characteristics compared to CBG solution. Furthermore, the freeze-drying process effectively addressed the issues of leakage and stability reduction during storage.[44,45]

The Albumin Nanoparticles

Albumin is a multifunctional protein nanocarrier with advantages such as biodegradability, biocompatibility, non-toxicity and non-immunogenicity.[69] In 2005, the FDA first approved albumin NPs containing the anticancer drug paclitaxel for the treatment of metastatic breast cancer.[70] As TS/TV and its active ingredients are known for rapid blood clearance and toxic side effects at high concentrations, maintaining low drug concentrations in the body over an extended period

remains a significant challenge. To address this, Su et al[46] prepared CBG- loaded bovine serum albumin (BSA) NPs (Cino-BSA-NP) using an aqueous desolvation process to investigate their therapeutic effect on liver cancer. The average particle size, zeta potential, EE and DL were 86.3 nm, −49 mV, 79.50% and 24.13%, respectively. Studies in SMMC-7721-bearing mice showed that treatment with Cino-BSA-NP significantly prolonged survival time. Additionally, acute animal experiments and histopathological examinations indicated that the nano-delivery system could reduce the toxicity of CBG. These results suggest that the controlled release of Cino-BSA-NP maintains CBG within a safe range, enhancing efficacy while reducing toxicity. Moreover, the nanocarrier minimizes direct drug interaction with blood and extends circulation time in the body. Similarly, Bufalin-BSA NPs prepared by Zhang et al[47] exhibited comparable characteristics, with a cumulative release of 59.16% in the first 3 hours of in vitro release, followed by a slow release and a gradual increase to 100% at 6-8 hours, demonstrating excellent controlled release properties. Compared to the BU group, Bufalin-BSA-NPs showed an extended half-life, reduced clearance rate, increased LD_{50}, enhanced hepatic cells uptake, and reduced cardiac and hepatic toxicity, along with significantly improved in vivo antitumor efficacy. These promising outcomes highlight the potential of albumin NPs in the development of future TDDS.

The Polymer Microspheres

Microspheres (MS) are small spherical structures formed by dissolving or dispersing drugs within polymer materials, which can enhance drug utilization and bioavailability while reducing side effects.[71] The positive charge of PLGA can facilitate electrostatic interactions between the microspheres and negatively charged tissue or cell receptors, thereby increasing the residence time of the microspheres at the target site and enabling controlled drug release.[72] Based on the analgesic effect of BU, Long et al[48] prepared bufalin-PLGA MS to elucidate the drug's effect and mechanism of action. bufalin-PLGA MS exhibited a slow drug release profile, extending the duration of action in vivo (within 48 h, in vitro cumulative release rate: 26.2%). In vivo experiments using the acetic acid twist test, hot plate test and chronic constriction injury model demonstrated that bufalin-PLGA MS significantly prolonged the duration of analgesia (free BU/bufalin-PLGA MS: 4 h/3 days) and reduced the frequency of administration compared to free BU. Mechanistic studies revealed that BU directly interacts with the P2X7 receptor, thereby inhibiting the expression of TRPV1 and regulating inflammatory factors such as IL-1β, TNF-α, IL-18, and IL-6. However, in vivo studies of bufalin-PLGA MS have focused on only one animal model of neuropathic pain. It is known that there are many causes of cancer pain and animal experimental models of cancer pain. Therefore, it is necessary to select more appropriate and richer animal models to better elucidate the efficacy and mechanism of drugs. In addition, the transdermal drug delivery system developed into nano-gel and microneedle is more convenient than intraperitoneal injection of bufalin-PLGA-MS in clinical application, thus opening a new way for the treatment of cancer pain. Polylactic acid (PLA) is a biomaterial known for its excellent biocompatibility and biodegradability, non-toxicity, non-irritation, as well as its superior mechanical properties and processability.[73,74] Chen et al[49] developed the slow-release microspheres of TV using PLA as a carrier by the emulsification-solvent evaporation method. Microspheres exhibited a rounded appearance with a smooth surface and particle sizes ranging from 1 to 10 μm, achieving an average DL of 23.4%. However, the precise mechanisms of action for these microspheres remain unclear. Further investigation using advanced techniques such as Western blotting, RT-qPCR, immunohistochemistry, and other related experimental methods is required to elucidate the underlying mechanisms and validate their therapeutic efficacy.

The Polymer Micelles

Polymer micelles are nanoscale assemblies formed by self-assembly of amphiphilic polymers with a core-shell structure in a straightforward manner.[75] Hydrophobic drugs are encapsulated within the hydrophobic core of these micelles, shielding them with an external hydrophilic shell. This shielding prevents the micelles from being eliminated by the mononuclear phagocytic system during circulation in the body, thereby extending the drug's circulation time. In addition, polymer micelles also have the characteristics of improved bioavailability and good biocompatibility. Therefore, polymer micelles are of great interest in TDDS.[76–78] Jing et al[50] prepared BU-micelle inclusion complex by co-precipitation, which is an amphiphilic dendritic polymer-based delivery system that can solve the problems of poor water solubility and tissue deposition characteristics of BU. The critical micelle concentration was determined to be 105.38 $\mu \cdot mol^{-1}$, with

micelle size of 130 nm. The results of BU solubility experiments indicate a significant increase in solubility when using lipidized dendritic polymers compared to saturated BU aqueous solutions. Liu et al[51] studied the preparation process of TV polymeric micelles by film dispersion method and micro-jet method, and finally determined that the average particle size of the polymeric micelles under the optimal process was 120 nm, and the encapsulation rate was as high as 94.12%. Yuan et al[52] prepared ABG-loaded polymeric nanomicelles with methoxy poly (ethylene glycol) (mPEG)-PLGA (ABG-PNs). ABG-PNs could facilitate the systemic delivery of ABG in vivo by increasing its water solubility. Furthermore, nanomicelles could enhance the anticancer effect of ABG by increasing cellular uptake.

The Liposomes

Liposomes refer to microvesicles formed when drugs are encapsulated by lipid bilayers. Liposomes are characterized by good biocompatibility, slow and long-acting effects, reduced drug toxicity and improved drug stability.[79] Furthermore, the use of liposomes as drug carriers enables transmembrane transport and provides selective passive targeting of tumor tissues.[80,81] Shen et al[53] prepared bufotenines liposomes with mean particle size, PDI and zeta potential of (130.1 ± 4.06) nm, 0.217 and (−8.00 ± 0.88) mV, respectively. The anti-inflammatory and analgesic effects of drug-loaded liposomes were proved by formalin-induced inflammatory pain behavior and hot plate experiments. In addition, the reduction of gastrointestinal stimulation by bufotenines is attributed to the down-regulation of cyclooxygenase and lipoxygenase in the lipid metabolism pathway and the up-regulation of cytochrome P450. Gao et al[54] developed BU derivative (BF211)-loaded PEGylation liposomes (BF211@Lipo), and optimized its formulation by QbD method to make it have the longest half-life time and EE up to (93.24 ± 2.15) %. After optimization, BF211@Lipo could prolong blood circulation time, reduce cardiotoxicity, and improve tolerance. Additionally, BF211@Lipo in combination with P188 was demonstrated to exert a more potent antitumor effect in HepG2 tumor-bearing mice than BF211(aq) alone, offering comparable or even superior therapeutic efficacy while reducing the dose of chemotherapeutic agents (Figure 2). Yuan et al[55,56] prepared PEG liposomes loaded with BU (BU-PEG-LPs). The half-life and AUC of BU-PEG-LPs were 1.61 times and 2.41 times that of those without PEG liposomes, respectively, indicating that PEGylation could prolong the action time of the drug in vivo and resist drug clearance. Acute toxicity evaluation and biological distribution showed that acute toxicity and cardiotoxicity were reduced. Sun[57] prepared long-circulating nanoliposomes of TV extract (TVE-LPs). The half-life in vivo and the total amount of drugs in liver and lung organs were higher than those of ordinary liposomes and raw material solutions, indicating that the long-circulating liposomes can prolong the action time of drugs in vivo and enhance target enrichment. Wu[58] developed PEG-modified long-circulating liposomes of BFN (BU-PEG-LIP). Pharmacokinetic experiments showed that the AUCs of BU, CBG and RBG were 1.68, 1.92 and 1.83 times higher, respectively, than those of unmodified PEG. Additionally, BU-PEG-LIP significantly prolonged the half-life in vivo.

The Emulsion

Nano-emulsions are typically heterogeneous systems composed of oil and water, characterized by good transparency, a large specific surface area, high stability and adjustable rheological properties.[82] Besides, nano-emulsions can improve the bioavailability and stability of lipophilic drugs,[83] making them widely used in delivery systems. Based on the theory of "unification of drugs and excipients", Li et al[59] prepared a nano-emulsion (TSE-BJO NEs) loaded with TS extract (TSE) and brucea oil (BJO). TSE-BJO NEs improved the rapid elimination of lipid soluble active ingredients in the body, enhanced the accumulation of drugs at the tumor site, and prolonged the retention time of drugs in the body. In HepG2 nude mice model, the TIR of TSE-BJO NEs was about 70% higher than the single drug-loaded NEs group, showing a good synergistic antitumor effect. Similarly, microemulsions have also been extensively studied for modulating the physicochemical properties of drugs and drug release kinetics.[84] Li et al[60] prepared a microemulsion loaded with BU, demonstrating high DL and EE, long-term stability and slow-release characteristics. Cytotoxicity assay revealed that the toxicity of the drug-loaded microemulsion was 1.4 times higher than that of pure BU suspension. In addition, pharmacokinetic studies in vivo demonstrated the retention time of BU prolonged in the blood.

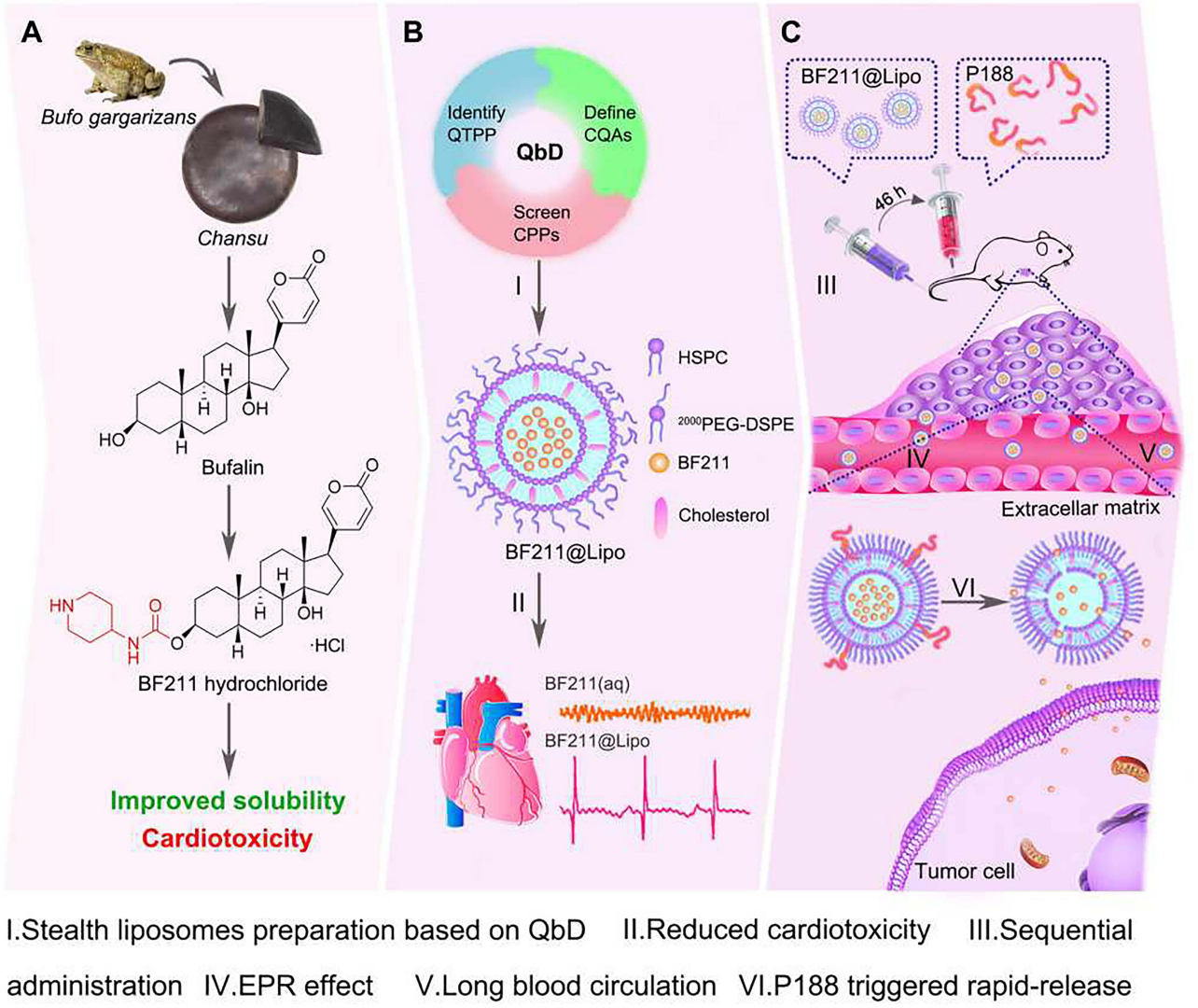

Figure 2 Schematic representation of liposomal BF211 and surfactant-assisted rapid release technologies for enhanced antitumor efficacy and reduced cardiotoxicity. (A) The evolution of bufalin derivatives from natural active ingredients through chemical modification. BF211 manifests the improved solubility and the remaining cardiotoxicity. (B) Stealth liposomal BF211 (BF211@Lipo) fabricated based on the Quality by Design (QbD) strategies for the prolonged blood circulation time and reduced cardiotoxicity. (C) Sequential injection of BF211@Lipo and P188 achieves surfactant-assisted rapid-release of liposomes, further boosting the antitumor efficiency. Reproduced with permission Dove Medical Press. Gao L, Zhang L, He F et al. Surfactant Assisted Rapid-Release Liposomal Strategies Enhance the Antitumor Efficiency of Bufalin Derivative and Reduce Cardiotoxicity. *International journal of nanomedicine*. 2021;16:3581–3598.[54]

Active Targeted Drug Delivery System

The active targeted drug delivery system primarily utilizes the surface modified ligands on nanocarriers to specifically bind to the highly expressed receptors on the surface of target cells, subsequently, the receptor-mediated endocytosis leads to the selective accumulation of drug-loaded NPs in target cells, thereby reducing the accumulation of drugs in non-target cells, minimizing toxicity, and enhancing efficacy. Receptor-ligand binding exhibits characteristics such as high specificity, selectivity, saturation, strong affinity, and significant biological effects.[85] At present, the commonly used ligands are small molecules, nucleic acid aptamers, peptides, antibodies, etc. Moreover, cell-based targeting strategies mainly rely on two biological principles: immune evasion and inherent tropism to target tissues. Specifically, the cell membrane-coated TDDS can be recognized as "self" by its own special membrane proteins instead of being eliminated, so that the drug is not removed, and specific cell types can perceive changes in the microenvironment of target regions, achieving specific targeted delivery.[86]

Subsequently, we primarily discuss the realization of active targeting through ligand or antibody modification and transmembrane camouflage.

Active Targeted System Based on Ligands or Antibodies Modification

Ligands/antibodies play a crucial role in distinguishing pathological from normal tissues by specifically binding to receptors/antigens overexpressed on the surface of cancer cells, minimizing damage to normal cells and exhibiting high cell selectivity.[87] Common biological ligands include protein or peptide antibodies, hyaluronic acid, folate, etc. This article focuses on constructing TDDS for TS/TV and its active components in cancer treatment, based on Integrin $\alpha_v\beta_3$, Asialoglycoprotein, Low Density Lipoprotein, Bile Acid, Folate, Transferrin, Epidermal Growth Factor, Biotin receptors and CD40 receptors. The related key points have been summarized in Table 2.

Integrin $\alpha_v\beta_3$ Receptor

Integrins serve as major cell adhesion receptors, regulating processes such as cell adhesion, migration, proliferation, spreading and apoptosis.[107] Consequently, integrin $\alpha_v\beta_3$ has garnered attention as a therapeutic target for numerous cancer types. Cyclic (arginine-glycine-aspartic acid peptide) (RGD) specifically binds to the highly expressed receptor integrin $\alpha_v\beta_3$ on vascularized endothelial cells, enhancing the tumor accumulation of the drug for better efficacy. Yuan et al[88] prepared a multifunctional delivery system for BU (BU@VeC/T-RGD MM) by grafting vitamin E succinate-grafted chitosan oligosaccharide (VES-CSO) and RGD-TPGS, aiming to enhance the therapeutic effect on drug-resistant colon cancer. In vitro, the drug-loaded mixed micelles showed excellent stability, sustained release characteristics, increased apoptosis and inhibited P-gp expression, which may be attributed to the ability of VES-CSO and TPGS to enhance solubility, stability and mitochondrial targeting properties. Compared to BU alone in vivo, BU@VeC/T-RGD MM had a more pronounced tumor inhibitory effect due to the EPR effect and RGD-mediated tumor targeting (65% vs 22%). On this basis, the team further investigated the inhibitory effect of the mixed micelle on intraperitoneal metastasis of ovarian cancer. BU@VeC/T-RGD MMs (BU@MMs) exhibited stronger inhibition of proliferation, promotion of apoptosis, and inhibition of migration and invasion in A2780 and SKOV3 ovarian cancer cells compared to free BU. Meanwhile, BU@MMs demonstrated enhanced inhibition of ovarian cancer cell metastasis, reduced toxicity and fewer side effects in the ID-8-bearing model. Moreover, the levels of EMT and ECM-related proteins in the serum of mice also showed a significant decrease trend, further verifying the effective inhibition of ovarian cancer metastasis by the mixed micelle in vivo (Figure 3).[89] Feng[90] prepared VES-COS/TPGS-RGD hybrid micelles loaded with BU (BUF@VeC/T-RGD MM), which exhibited a slow release profile after a 1-hour sudden release. The slow release of the drug from the BUF@VeC/T-RGD MM prolonged the action time in vivo, and the hybrid micelles also exhibited stronger uptake and growth inhibition in LoVo cells. Yin et al[91] also prepared RGD-modified BU-loaded NPs (BNPs) and demonstrated that RGD modification can improve cell uptake, enhance tumor targeting, prolong in vivo action time (the mean residence time was prolonged from 3.45 h to 7.63 h) and enhance antitumor effect. Furthermore, RGD-modified PEGylated liposomes loaded with BU (L-RGD-PEG-BF) were developed by Zhang et al.[92] The cell survival rate of L-RGD-PEG-BF is lower, compared to unmodified liposomes. The IC_{50} value of L-RGD-PEG-BF was 2.36 times lower than free BU. L-RGD-PEG-BF exhibited higher cytotoxicity, apoptosis rate, and uptake properties in A549 cells compared to untargeted liposomes and free BU. All of the above studies demonstrated that the prepared nanocomplexes have better tumor targeting because RGD peptide can specifically bind to integrin $\alpha_v\beta_3$ receptor.

Asialoglycoprotein Receptor

Asialoglycoprotein receptor (ASGPR), a member of lectin family, is widely expressed in liver cells.[108] It also has high affinity for carbohydrates, particularly galactose, N-acetyllactosamine and glucose, and promotes uptake through clathrin-mediated endocytosis.[109] Consequently, ASGPR-modified NPs have been extensively studied for active targeting of liver cancer. Dong et al[93] first synthesized galactosyl-succinyl-poloxamer 188-polylactic acid-glycolic acid copolymer (Gal-SP188-PLGA), which was used to prepare RBG-loaded NPs (RGPPNs). Galactosyl residues can specifically bind to ASGPR for targeted drug delivery to the liver. The RGPPNs exhibited stronger cytotoxicity and cellular uptake in vitro

Table 2 Active TDDS Based on Ligands or Antibodies Modification of Active Ingredients of TS/TV

Name	Ligands/Antibodies	Receptor/Antigen	Characterization	Pharmacokinetics/Tissue Distribution/Efficacy	Diseases	Ref., Year
BU@VeC/T-RGD MM	RGD	$\alpha_v\beta_3$	Size: (140.3±0.8) nm PDI: 0.19 Zeta potential: (8.66±1.07) mV LE: 2.24%	Cellular uptake in LoVo/ADR cell↑; Cytotoxicity in HCT116/LOHP and LoVo/ADR cells: BU@VeC/T-RGD>BU@VeC/T>BU@VeC>BU	Colon cancer	2018[88]
BU@MMs	RGD	$\alpha_v\beta_3$	Size: (161±1.4) nm PDI: 0.17 Zeta potential: (4.49±1.54) mV DL: 2.54%	The IC_{50} values in A2780 and SKOV3 cells: Free BU>BU@MMs; The apoptosis rate of A2780 and SKOV3 cells: BU@MMs>Free BU>VeC/T-RGD MM>Ctrl; Inhibition rate in ID8 cell peritoneal metastasis model in C57BL/6 mice↑	Ovarian cancer	2023[89]
BUF@VeC/T-RGD MM	RGD	$\alpha_v\beta_3$	Size: 140.3 nm PDI: 0.19 Zeta potential: (8.66±1.07) mV DL: 2.24%	Cellular uptake in LoVo cells↑; Cytotoxicity in LoVo cell↑	Cancer	2021[90]
BNPs	RGD	$\alpha_v\beta_3$	Mean Size: (164±84) nm PDI: 0.209 Zeta potential: 2.77 mV EE: (81.7±0.89) % DL: (3.9±0.16) %	Cellular uptake in HUVEC cells: Rb-mPEG-PLGA-PLL-cRGD NPs>Rb-mPEG-PLGA-PLL NPs; After 32 hours postinjection, the tumor fluorescence intensity of mice: Rb-mPEG-PLGA-PLL-cRGD NPs>Rb-mPEG-PLGA-PLL NPs; Inhibition of tumor in colon cancer-bearing mice: BNPs>Free BU Pharmacokinetics: AUC, $t_{1/2}$, V↑	Colon cancer	2012[91]
L-RGD-PEG-BF	RGD	$\alpha_v\beta_3$	Mean Size: (87.9±3.9) nm PDI: 0.20 Zeta potential: (−19~−21) mV EE: (90.6±4.98) %	The IC_{50} values in A549 cell: L-BF>L-PEG-BF>L-RGD-PEG-BF; Apoptosis of A549 cell↑	Lung cancer	2019[92]
RGPPNs	Galactose	Asialoglycoprotein	Size: (100~200) nm	Cellular uptake in the HepG2 cells↑; Liver functional indexes in the serum and liver of the primary hepatocarcinogenic mice: ALT, AST, c-GT, T-BIL↓	Liver cancer	2017[93]
BU-LP-NPs	Low density lipoprotein	Low density lipoprotein receptor	Mean Size: (82.4±28.5) nm PDI: 0.120 Zeta potential: −19.44 mV	Delayed release in vitro	—	2016[94]

BF-uPPNCs	Ursodeoxycholic Acid	Bile acid	Mean Size: (155.2±5.3) nm PDI: 0.195 Zeta potential: (−10.08±2.53) mV EE: (69.2±3.1) %	The inhibition effect on tumor HepG2 cells↑; The inhibition rate in bearing H22 mice: BF-uPPNCs>BF-PNPs>Free BU Pharmacokinetics: MRT, $T_{1/2}$, AUC↑	Liver cancer	2021[95]
BF-ND-BUP-sMPs	Ursodeoxycholic Acid	Bile acid	DLS: 879±56 nm PDI: 0.16 Zeta potential: (−5.86±1.12) mV EE: BF/ ND: 78.0%/76.2%	The IC_{50} values of HepG2 cells: BU-ND -P-sMPs>BU-ND-UP-sMPs>BU-ND-BP-sMPs> BF-ND-BUP-sMPs; Cellular uptake on the HepG2 cell↑; Anti-tumor effect: BF-ND-BUP-sMPs >BU-ND-BP-sMPs>BU-ND-UP-sMPs>BU-ND-P-sMPs	Liver cancer	2021[96]
PB/PCTm	Taurocholic acid	Na^+-tauro-cholate co-transporting polypeptide	a: PTX/PCTm, b: BF/PCTm Mean size: a: (114.63±1.56) nm, b: (163.73±7.20) nm PDI: a: (0.180±0.023), b: (0.228 ±0.027) Zeta potential: a: (−4.32±0.489) mV, b: (−6.28±0.545) mV EE: a: (93.41±4.34) %, b: (82.25 ±3.38) % DL: a: (9.51±0.40) %, b: (2.41 ±0.09) %	The inhibition rate of bearing HepG2 cell mice: PB/PCTm>BF/PCTm>PTX/PCTm>Taxol; The apoptosis rate of tumor tissue↑	Liver cancer	2022[97]
FA-CS-L	Folate	Folate receptor	Mean Size: (160±13) nm Zeta potential: (4.0±1.1) mV PDI: (0.154±0.013) EE: BU/CBG/RBG: (95.11 ±0.21)%/(97.35±0.02)%/(93.52 ±0.56)%	The 48 h survival rate of HeLa cells↓; Cytotoxicity in HeLa cell↑	Cancer	2017[98]
FA/BF/β-CD	Folate	Folate receptor	EE: (94.22±0.85) % DL: (14.11±0.20) %	Survival rate of HCT116 cells: pure BU>BF/β-CD inclusion complex>FA/BF/β-CD inclusion complex; Cellular uptake on HCT116 cells↑	—	2017[99]
FA-BF-CLs	Folate	Folate receptor	Mean Size: (135.5±1.40) nm PDI: (0.192±0.025) Zeta potential: (16.23±0.46) mV EE: (69.42±2.18) %	Drug release↓; In vitro cytotoxicity on HepG2 cell: FA-BF-CLs>BF-CLs, Free BU	Liver cancer	2023[100]

(*Continued*)

https://doi.org/10.2147/IJN.S469742

Table 2 (Continued).

Name	Ligands/Antibodies	Receptor/Antigen	Characterization	Pharmacokinetics/Tissue Distribution/Efficacy	Diseases	Ref., Year
Le/Bu@mSiO$_2$-FA	Folate	Folate receptor	Size: 113 nm DL: Le/BU: 16.4%/17.4%	Cellular Uptake on 9810 cells↑; The IC_{50} values of 9810 cells: Lenvatinib/Bufalin>Bu@mSiO$_2$-FA>Le@mSiO$_2$-FA>Le/Bu@mSiO$_2$-FA; Tumor growth of CCA in vivo↓	cholangiocarcinoma	2022[101]
(FA+Tf) BF-LPs	Transferrin, folate	Transferrin receptor, Folate receptor	Mean Size: 120.4 nm PDI: 0.121 Zeta potential: −16.8 mV EE: 82.3% DL: 10.7%	The IC_{50} values of 9810 cells: Blank LPs> Free BU>BF-LPs>FA-BF-LPs>Tf-BF-LPs>(FA+Tf) BF-LPs; Cellular uptake on A549 cells↑; In vivo optical imaging of xenografts: (FA+Tf) BF-LPs>Tf-BF-LPs>FA-BF-LPs>Blank LPs; Tumor growth rate in transplanted A549 cells mice↓	Lung cancer	2018[102]
Bufalin-CaP/DPPE-PEG-EGF NSs	EGF	EGFR	Mean Size: 171 nm EE: 83.2%	Cellular Uptake on HCT116 cells↑; Cytotoxicity in HCT116 cells: Bufalin-CaP/DPPE-PEG-EGF NSs>Bufalin-CaP/DPPE-PEG NSs; In Vivo Tumor-Targeting rate↑; The apoptosis rate of HCT116 cell in model nude mice: Bufalin-CaP/DPPE-PEG-EGF NSs>Bufalin-CaP/DPPE-PEG NSs>Free BU>saline group	Colon cancer	2019[103]
BU-Me@Ce-LPs	Cetuximab	EGFR	Size: (146.51±8.63) nm Zeta potential: (9.03±0.25) mV	Killing effect and apoptosis of SMMC-7721-R cells↑	Liver cancer	2019[104]
Bu-BCS-NPs	Biotin	Biotin receptor	Size: (171.6±31.3) nm Zeta potential: +16.5 mV EE: ~ 77.4% DL: ~ 13%	IC_{50} values of Bu-BCS-NPs/Free BU on MCF-7 cell: 0.582/1.896 μg/mL Cell uptake↑; Drug release↓	Breast cancer	2014[105]
Anti-CD40-BFL	Anti-CD40	CD40	Mean Size: (205.4±68.4) nm PDI: 0.062 Zeta potential: −15.86 mV EE: (73.59±3.14) %	Tumor growth inhibition in C57/BL6 mice: anti-CD40-BFL>Free BU; The apoptosis of B16 cells↑	Melanoma	2014[106]

Abbreviations: EE, encapsulation efficiency; DL, drug load efficiency; LE, loading efficiency; PDI, polydispersity index; AUC, area under the curve; MRT, mean residence time; $t_{1/2}$, half-life; C_{max}, maximal concentration; T_{max}, time of maximum concentration; V, apparent volume of distribution; BU, bufalin; CBG, cinobufagin; RBG, resibufogenin; ABG, arenobufagin; CBF, cinobufotalin; ALT, alanine aminotransferase; AST, aspartate aminotransferase; c-GT, γ-glutamy transpeptidase; T-BIL, Total bilirubin.

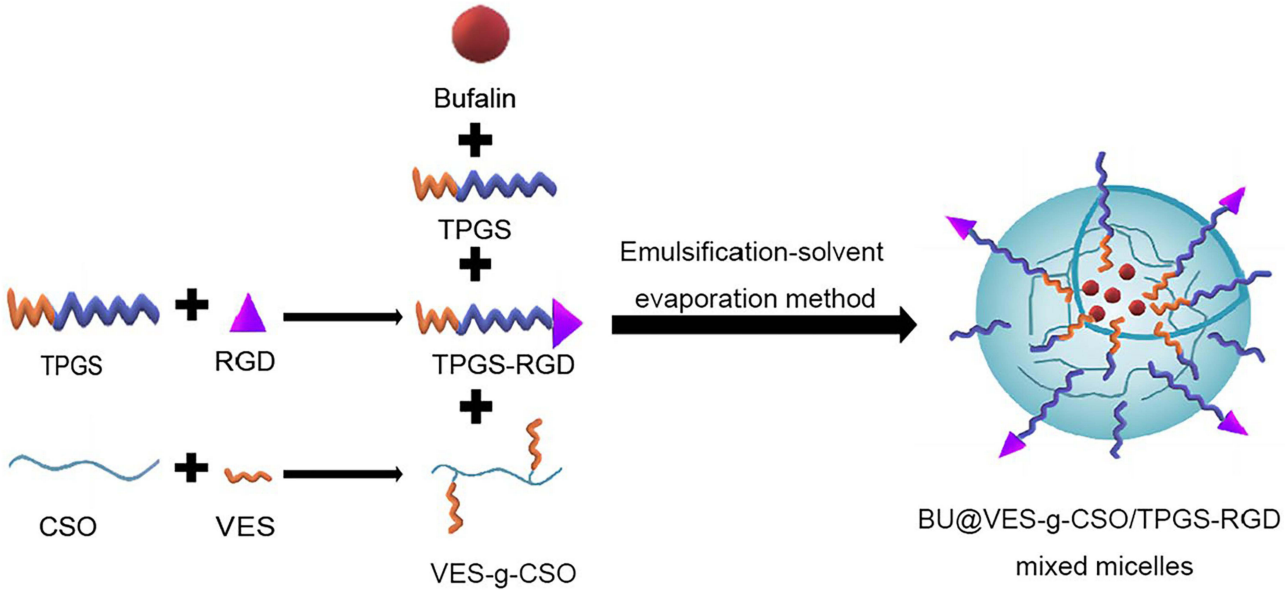

Figure 3 BU@MMs formulation mechanism Reproduced from Xu, L., Ma, S., Fan, B. et al. Bufalin-loaded vitamin E succinate-grafted chitosan oligosaccharide/RGD-conjugated TPGS mixed micelles inhibit intraperitoneal metastasis of ovarian cancer. *Cancer Nano* 2023, 25. Creative Commons.[89]

studies compared to other groups. Simultaneously, RGPPNs also showed improved serum and liver homogenate indicators than the other groups, reflecting its favorable therapeutic effect in vivo.

Low Density Lipoprotein Receptor

Lipoprotein, as an endogenous protein particle, has good biocompatibility and safety, and can target the overexpressed low density lipoprotein receptor (LDLR) on the surface of some tumors, thus garnering extensive attention.[110] Li et al[94] prepared BFN-loaded lipid protein hybridization NPs (BU-LP-NPs) with round and uniform appearance, an average particle size of (82.4 ± 28.5) nm, and a zeta potential of −19.44 mV. By exploiting the properties of LDLR, which is overexpressed by tumor cells, BU-LP-NPs were able to achieve better tumor targeting of the drug. DSC and X-ray results demonstrated that the drug existed in amorphous form in the formulations. Compared to the solution, BU-LP-NPs could significantly delay the release of the drug, with no burst release observed in vitro, thereby initially addressing the challenge of the short half-life and rapid elimination of BFN.

Bile Acid Receptor

Bile acids (BAs) are synthesized from cholesterol in the liver and are regulated by the farnesol X receptor (FXR) and the G protein-coupled BA receptor 1 (GPBAR1/TGR5), which can be taken up by hepatocytes and have a targeted effect on the liver.[111] Xu et al[95] prepared ursodeoxycholic acid (UA) modified BSA-PBCA NPs loaded with BU (BF-uPPNCs). Since UA can enhance carrier targeting through the bile acid transporter overexpressed in liver and intestine tumors and improve the transcytosis of tumor cells, in vivo studies showed that BF-uPPNCs exerted the best antitumor effect compared to free BU and unmodified PBCA NPs with UA. Additionally, the team also prepared albumin sub-microspheres with a core-shell structure modified by biguanide and UA to co-deliver BU and nintedanib (BF-ND-BUP-sMPs). The fluorescence intensity of BF-ND-BUP-sMPs was the strongest, being 1.4 times higher than unmodified. Compared with other groups, BF-ND-BUP-sMPs showed the strongest in vivo antitumor effect (TIR: 84.2%), suggesting that BF-ND-BUP-sMPs had the strongest tumor targeting ability.[96] Polymer micelles (PB/PCTm) co-loaded with the Chinese medicines BU and paclitaxel (PTX) were also designed to increase drug solubility, prolong in vivo circulation time and achieve hepatic targeting by using the amphiphilic block copolymer mPEG and cholic acid. PB/PCTm were targeted to hepatocytes via Na^+-taurocholate co-transporting polypeptide receptors, thereby enhancing cellular uptake. In vivo imaging showed that PB/PCTm still had strong fluorescence intensity within 48 h. In addition, the TIR of HepG2-

bearing mice was as high as 82.29% and the positive rate of Ki67 was only 8.16%, which was the strongest inhibition of cell proliferation and showed no obvious systemic toxicity.[97]

Folate Receptor

As one of the most widely used receptors for active targeting, the folate receptor has several advantages, including low immunogenicity, rapid tumor penetration, high affinity for a wide range of tumors, chemical stability, and easy production.[112] Moreover, unlike folate entering normal cells through transmembrane action, folate will specifically bind to folate receptors on the surface of cancer cells to form folate complexes, which then form endocytotic vesicles that enter cancer cells by internalization.[113] Guo et al[98] prepared folate receptor-targeted long-circulating liposomes loaded with toad venom extract (FA-CS-L) by thin-film dispersion method. For HeLa cells with high expression of folate receptor, the long-circulating liposomes modified by folateshowed a stronger inhibitory effect on cell proliferation, indicating that FA-CS-L could effectively bind to the folate receptor on the surface of the tumor and make the drug accumulate more in the tumor tissue and exert a stronger tumor inhibitory effect. Zou et al[99] prepared a folate receptor-targeted BU/β-cyclodextrin (β-CD) supramolecular inclusion complex (FA/BF/β-CD) to improve the solubility and antitumor efficacy of BU. In HCT-116 cells, the IC_{50} value of FA/BF/β-CD was approximately 2.2 times higher than that of the non-targeted inclusion complex and pure BU. And the inclusion complex had higher drug uptake than non-targeted inclusion complex. Luo et al[100] prepared folate modified BU cationic liposomes (FA-BF-CLs). The HepG2 cell activity of FA-BF-CLs was significantly lower than unmodified, which was attributed to the folate carried by FA-BF-CLs binding to the folate receptor on the HepG2 cell membrane and mediating the intracellular transport of the carrier through receptor-mediated endocytosis, thereby releasing the drug. A silica NPs sequentially modified with PEG and folate was prepared to co-deliver lenvatinib (Le) and BU (Le/Bu@$mSiO_2$-FA) to target cholangiocarcinoma (CCA). Le/Bu@$mSiO_2$-FA was able to reduce CCA cell migration and invasion. Furthermore, Le/Bu@$mSiO_2$-FA significantly inhibited tumor growth in 9810 bearing mice, compared with Le and BU alone.[101]

Transferrin and Folate Receptor

Compared to normal cells, cancer cells have a higher demand for iron to support their rapid proliferation, and transferrin (Tf), which acts as an iron carrier, is overexpressed on the surface of cancer cells. Therefore, transferrin-modified nanocarriers can enhance the specificity of drugs to cancer cells.[114] Chen et al[102] prepared Tf and FA co-modified BU liposomes [(FA+Tf) BF-LPs] for the treatment of lung cancer by high pressure homogenization. Due to the internalization of receptor-mediated surface-modified liposomes in tumor cells, (FA+Tf) BF-LPs were most effective against A549 cells. In addition, the fluorescence intensity of (FA+Tf) BF-LPs were was strongest under fluorescence microscopy, indicating enhanced drug release in tumor cells. (FA+Tf) BF-LPs showed the most significant inhibitory effect on tumor growth in xenografted A549 mice, and no systemic toxicity was observed in vivo.

Epidermal Growth Factor Receptor

The epidermal growth factor receptor (EGFR) is a transmembrane tyrosine kinase receptor that is overexpressed in a variety of epithelial-derived cancers, and its natural ligands include EGF and TNF-α. Cetuximab is a human-mouse chimeric monoclonal antibody with high affinity for EGFR.[115] Calcium phosphate (CaP)/1,2 bis(diphenylphosphino) ethane (DPPE)-PEG-epidermal growth factor hybrid porous nanospheres loaded with BU (Bufalin-CaP/DPPE-PEG-EGF NSs) were prepared by Xu et al[103] Bufalin-CaP/DPPE-PEG-EGF NSs could be internalized by HCT-116 cells through receptor-mediated endocytosis of EGF for tumor targeting. In tumor-bearing mice, Bufalin-CaP/DPPE-PEG-EGF NSs resulted in a significantly higher inhibition rate without significant weight loss compared to the non-targeted treatment group. Huang[104] constructed compound immunoliposomes (BU-Me@Ce-LPs) loaded with BU and melittin coupled with anti-HER1 monoclonal antibody cetuximab (Ce). BU-Me@Ce-LPs not only overcame the shortcomings of easy hemolysis of melittin and poor water solubility of BU, but also addressed the problem of poor specificity of liposome delivery drugs. Compared to HepG2 and Huh7 cells with medium and low expression of HER1, BU@Ce-LPs could have higher transfection efficiency and killing effect in SMMC-7721-R cells with high expression of HER1. Compared to non-targeted liposome and free drug, BU-Me@Ce-LPs had stronger therapeutic effect and better safety.

Biotin Receptor

Biotin, a water-soluble vitamin that plays an important role in cell growth, signaling, and numerous other cellular functions, is internalized into cells by binding to sodium-dependent multivitamin transporters (SMVT) on the cell surface.[116] Tian et al[105] loaded BU spirit of biotin was prepared chitosan NPs (Bu-BCS-NPs) to play a role of treatment of breast cancer. Bu-BCS-NPs exhibited stronger cytotoxicity against breast cancer MCF-7 cells than the native BU (IC_{50}: 0.582 vs 1.896 μg/mL). The intracellular uptake of Bu-BCS-NPs were observed to be faster and higher than that of non-modified CS NPs (Bu-CS-NPs), which may be attributed to the active internalization of Bu-BCS-NPs by transporters in the cell membrane, leading to increased uptake. Additionally, in vivo studies using the MCF-7 nude mouse tumor model confirmed the significant therapeutic effect of Bu-BCS-NPs.

CD40

Anti-CD40 is a member of the tumor necrosis factor (TNF) receptor superfamily that enhances antigen presentation and activates cytotoxic T-cells against less immunogenic tumors. Additionally, the receptor is expressed on the surface of a variety of cancer cells.[117] Li et al[106] designed an immune liposome (anti-CD40-BFL) co-delivered with BU and anti-CD40 antibodies to exert synergistic therapeutic efficacy. In vivo antitumor studies demonstrated that anti-CD40-BFL could prolong the release at the tumor site, compared to unmodified liposomes, while also preventing the entry of monoclonal antibodies into the systemic circulation, thus blocking systemic toxicity. In addition, apoptosis assays revealed that anti-CD40-BFL could exert potent antitumor effects through a mitochondria-dependent pathway.

Active Targeted System Based on Biological Membrane Coating

Biomimetic NPs improve their biocompatibility by incorporating a cell membrane onto NPs through cell membrane coating technology.[118] This approach utilizes cell membranes from various sources such as red blood cells, cancer cells, and white blood cells. By doing so, the resulting biomimetic nanocarriers gain self-recognition and homologous targeting capabilities, enabling more precise targeting of tumor tissues and prolonging circulation time in vivo. Additionally, they enhance immune evasion and cellular uptake, addressing issues related to premature clearance and nanocarrier toxicity.[119] The active targeted system based on biological membrane coating are summarized in Table 3.

Platelet Membrane

Platelets are participants in many biological functions and pathological conditions and are highly reactive cells that can adapt to environmental changes thereby releasing a wide range of biomolecules. Platelets are able to evade the immune system, subendothelial adhesion and pathogen interactions.[132] Wang et al[120] prepared platelet membrane(PLTM)-coated and BU-loaded, hollow MnO_2 NPs (PLTM-HMnO_2@Bu NPs) for cancer treatment. The results demonstrated that the H22 cells exhibited a high intake of Mn^{2+} content in the tumor in vitro and in vivo, with the concentration in the tumor being much higher than in other organs. The modified PLTM NPs had good ability to selective target tumors and to evade the immune system. Furthermore, the cell vitality of H22 cells was about 3 times less than free drug treatment group (34% vs 13%). In vivo, the PLTM-HMnO_2@Bu NPs treatment group showed the slowest tumor growth rate, the volume of the smallest and the highest level of apoptosis at tumor tissue. Moreover, the team also previously prepared[121] PLTM-coated BU-loaded chitosan oligosaccharide (CS)-PLGA NPs (PLTM-CS-pPLGA/Bu NP). Compared to the uncoated NPs, the PLTM-CS-pPLGA/Bu NP demonstrated enhanced absorption, with a fluorescence intensity in tumors that was 1.15 and 3.12 times higher than that in the liver and kidney, respectively, suggesting that the NPs exhibited good tumor targeting ability. In vivo PLTM-CS-pPLGA/Bu NP treatment showed the most powerful antitumor effect, with no adverse effects on major organs (Figure 4).

Erythrocyte Membrane

"Self-recognition" on the erythrocyte membrane protein exists to its low immunogenicity and longer cycle durability.[133] Fan et al[122] prepared a total of GBF and Dox bionic nanoparticle delivery systems (GTDC@M-R NPs) by erythrocyte membrane coating. In vitro experiments showed that the delivery system had a good biocompatibility, and prolonged the circulation of the blood (three times longer than GT NPs). In addition, the accumulation of GTDC@M-R NPs at the tumor site increased about 2 times compared to bare GTDC NPs, and the mean number of metastatic nodules in the lung

Table 3 Active TDDS Based on Cell Membrane Coating of Active Ingredients of TS/TV

Name	Membrane type	Characterization	Pharmacokinetics/Tissue Distribution/Efficacy	Diseases	Ref., Year
PLTM-HMnO2@Bu NPs	Platelet membrane	Mean Size: 187nm PDI: 0.171 Zeta potential: −27 mV EE: (93.6±2.6) % DL: (23.8±2.9) %	The IC_{50} values of H22 cell: Free BU>PLTM-HMnO_2@Bu NPs; Survival rate of H22 cell↓; PLTM-HMnO_2@Bu NPs have good tumor selectivity; The tumor growth of mice bearing H22 cells treated with PLTM-HMnO_2@Bu NPs was the slowest and the smallest.	Cancer	2020[120]
PLTM-CS-pPLGA/Bu NPs	Platelet membrane	Mean Size: 192 nm Zeta potential: ~−28 mV EE: (92.8±3.5) % LC: (8.5±1.9) %	Drug release: pH=5.5>pH=7.4; Cellular Uptake on H22 cells: FITC-PLTM-CS-pPLGA NPs>FITC-CS-pPLGA NPs; In vivo and vivo fluorescence imaging: tumor>liver>spleen; Anti-tumor effect of H22 tumor-bearing ICR mice in vivo↑	Cancer	2019[121]
GTDC@M-R NP	Erythrocyte membrane	Mean Size: 70 nm Zeta potential: −19.11 mV	Drug Release↓, Cell uptake↑, Cell viability of MDA-MB-231: GTDC@M-R NP>GDC@M-R NP>GTDC@M NP, Tumor inhibition rate of tumor-bearing mice↑	Triple-negative breast cancer	2020[122]
HA@RBC@PB@CS-6 NPs (HRPC)	Erythrocyte membrane	Size: 140 nm Zeta potential: −12.6 mV	Cell uptake↑; Immune evading ability↑; Circulation life↑ (HRPC vs PB, 7.5 h vs 2.3 h), TIR of HPRC+L in vivo: 93.4%	Breast cancer	2019[123]
CBAP	A549 cancer cell membrane.	—	The drug resistance of pancreatic cancer cells to GEM and 5-FU was reversed.	Pancreatic cancer	2023[124]
Cu_{2-x}Se-CB@MEM	Glioma cell membrane	Size: 132.5 nm Zeta potential: −22.7 mV	The killing effect of U87 cells and Ln229 cells: Cu_{2-x}Se-CB@MEM+L>Cu_{2-x}Se-CB@MEM>Cu_{2-x}Se-CB; Cellular Uptake on HUVEC cells↑; Apoptosis rate of Ln229 cells↑; Circulation life in the tumor bearing nude mice↑; Tumor growth in Ln229 glioma-bearing mice↓	Glioma	2023[125]
LP-R/C@AC	Erythrocyte membrane HGC-27 cell membrane	Mean Size: 108 nm Potential: 7.5 mV EE: AP/CBG: 94.2%/99.9%	Drug Release: pH=5.2>pH=7.4; The killing effect of HGC-27 cells↑; Drug release cycle↑; The apoptosis rate of HGC-27 cells: LP-R/C@AC>LP-R/C@C>LP-R/C@A; Anti-tumor in vivo: LP-R/C@AC>LP-AC>AC>AP>CBG	Gastric carcinoma	2021[126]

PC@M NPs	Erythrocyte membrane, SW480 cell membrane	Mean size: 185 nm Zeta potential: 12.87 mV EE: 57.55% DL: 11.5% (CS-1: PB=1:5)	Cell viability of SW480: Free CBG>PC@M NPs+L; cell apoptosis of SW480: PC@M NPs>Free CBG; Tumor inhibition rate of tumor model in vivo: PC@M NPs+L>PB@M NPs+L>PC@M NPs>PBS>Free CBG; Tumor inhibition rate of postoperative recurrence model of CRC: PC@M NPs+L>PB@M NPs+L>PC@M NPs>Free CBG	Colorectal cancer	2023[127]
CPCCM	Erythrocyte membrane, MDA-MB-231 cell membrane	Size: (30±5) nm Zeta potential: −14.9 mV EE: 76.53%	4T1 and MDA-MB-231 cell viability↓; Drug Release: pH=6.8>pH=7.4; cycle half-life↑; TIR↑; Tumor cell apoptosis in vivo↑	Triple-negative breast cancer	2022[128]
CS-1@PB[HM] NP	Erythrocyte membrane, MDA-MB-231 cell membrane	Mean size: (207±12) nm; Zeta potential: (−7.5±0.5) mV	The half-life in BALB/c mice↑; Fluorescence signal in tumor tissue: PB^{Ce6}[HM] NPs>Pure PB^{Ce6} NPs; Cytotoxicity of MDA-MB-231: CS-1@PB[HM] NP+L>PB[HM] NP+L	Triple-negative breast cancer	2023[129]
HM-PLGA@ GC&CS-6 NPs	Erythrocyte membrane MDA-MB-231/4T1 cells membrane	Size:122 nm Zeta potential: −15.6 mV	Cell uptake of RAW264.7↓; Cell uptake of MDA-MB-231↑; Blood circulation time↑	Triple-negative breast cancer	2022[130]
PCDI@M	Erythrocyte membrane Hela cell membrane	Mean size: 126.2±9.8 nm Zeta potential: −26.7±2.0 mV	Cell uptake of RAW264.7↓; Drug Release: pH=5.2 (52.3%)>pH=7.4 (14.2%); Blood half-life↑; TIR↑	Cervical cancer	2021[131]

Abbreviations: EE, encapsulation efficiency; DL, drug load efficiency; PDI, polydispersity index; TIR, tumor inhibition rate.

https://doi.org/10.2147/IJN.S469742

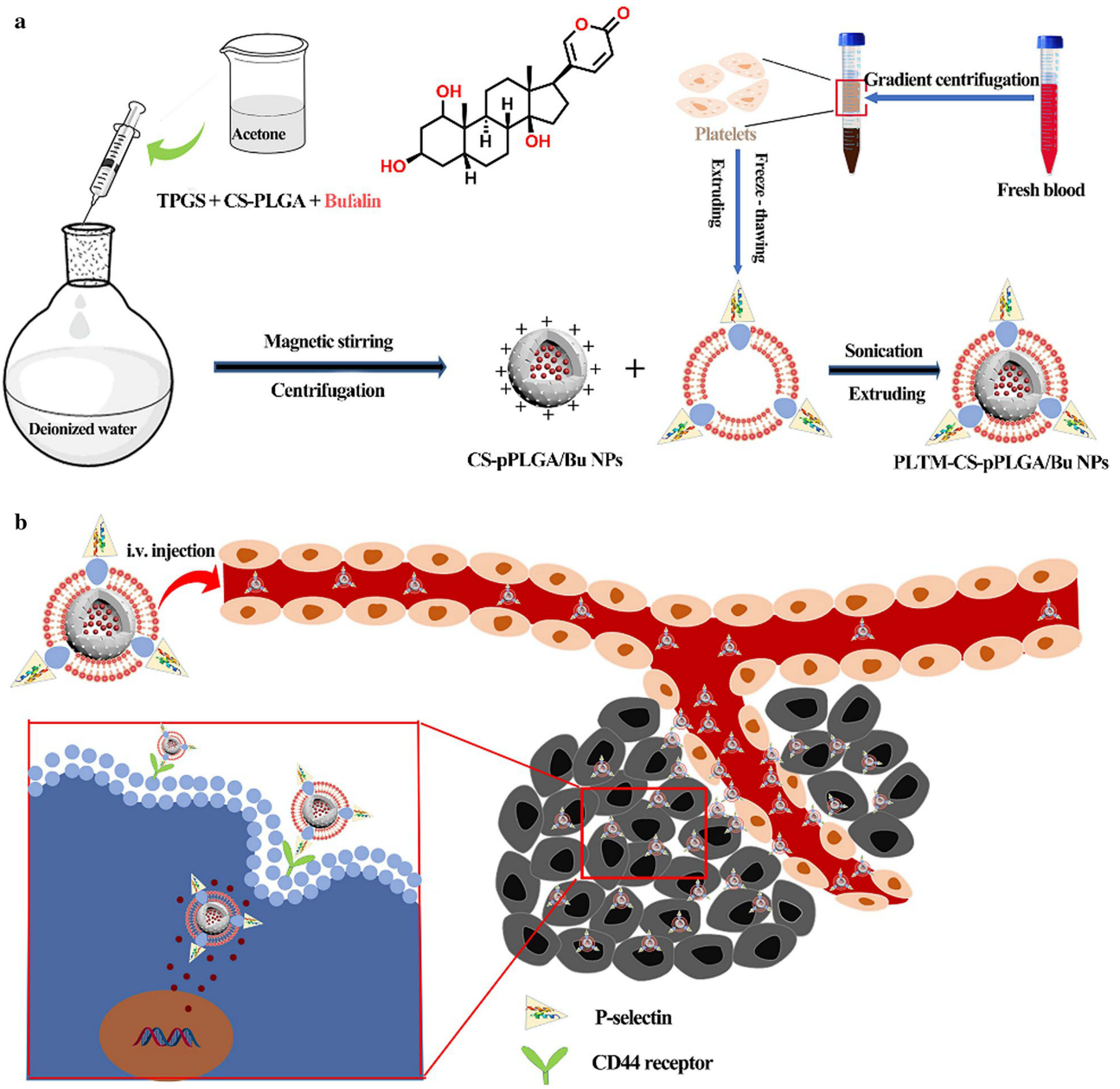

Figure 4 (**a**) Illustration of the preparation route to PLTM-CS-pPLGA/Bu NPs; (**b**) In vivo targeted bufalin delivery to a tumor site mediated by binding of P-selectin on the surface of the PLTM to CD44 receptors of the tumor cells. Reproduced with permission from reference Reproduced from Wang H, Wu J, Williams GR et al. Platelet-membrane-biomimetic nanoparticles for targeted antitumor drug delivery. *J Nanobiotechnology*. 2019;17(1):60 Creative Commons.[121]

of tumor-bearing mice was reduced by 84% compared with controls. Liu et al[123] constructed red cell membrane coated GBF-loaded hollow porous Prussian blue NPs (HA@RBC@PB@CS-6 NPs, HRPC) for the treatment of breast cancer. The signal intensity of HRPC was 1.67-fold higher than that of RPC or PC treatment groups in cellular uptake experiment, which demonstrated the selective accumulation of HRPC at the tumor site. CD47 on the erythrocyte membrane could help the NPs to reduce macrophage recognition in vivo, which could in turn increase the cycling lifetime of the NPs. In addition, the half-life of HRPC than PB increased 3.3 times (7.5 h vs 2.3 h) also proves this point in vivo.

Cancer Cell Membrane

Based on the immune escape and homologous adhesion capacity of cancer cells, novel drug delivery systems have the potential to overcome the dilemma of immune clearance and non-specific binding by encapsulating the cancer cell membrane.[134] The use of corresponding cancer cell membrane coating for different cancers can improve the precise targeting of drugs to tumor tissues.

Pancreatic Cancer Cell Membrane

Zhang et al[124] developed BU-loaded poly (lactic-co-glycolic acid) (CBAP) NPs camouflaged with cancer cell membranes to investigate their potential in reversing chemoresistance in pancreatic cancer. The membrane-coated blank NPs exhibited higher accumulation at the tumor site, highlighting the tumor-targeting properties of the nanocarrier, which supports increased drug accumulation at the tumor site. In addition, the blood biochemical analysis indicated that CBAP did not induce cardiotoxicity, suggesting that the membrane coating mitigates the cardiotoxic effects of BU. In the mouse model, CBAP in combination with various chemotherapeutic agents for pancreatic cancer significantly reduced the tumor weight but essentially unchanged the body weight of the mice as compared to monotherapy, which not only demonstrated the good reverse translational drug resistance but also the good safety profile of CBAP.

Glioma Cell Membrane

Song et al[125] developed a highly efficient biomimetic nanocomposite loaded with CBF ($Cu_{2-x}Se$-CB@MEM, CCM). In the Ln229-luc model with the CCM treatment group, not only did it have the highest fluorescence intensity in isolated brain tissue, but it was also 1.5 times higher than that of the CC group, suggesting that BBB receptors can recognize homologous glioma cell tumor through ligand-receptor interactions and enhance drug entry into tumor cells through homologous targets. In addition, the CCM-treated group showed smaller tumor size and further inhibition of tumor growth (32 days) when combined with NIR therapy, suggesting a synergistic effect of combining chemotherapy with PTT. This means that in the future we can take advantage of the excellent targeting ability of this drug and combine it with photothermal therapy to increase its value.

Erythrocyte and Cancer Cell Membrane

The aforementioned biomimetic targeted delivery systems formed by a single cell membrane have demonstrated all the excellent characteristics with some inherited advantages, but at present, hybrid membranes formed by combining two or several different cells exhibit even more incredible vitality. For example, hybrid membranes formed from erythrocyte and membranes of different tumor cancer cells can be used to provide targeted drug delivery systems that offer either lower immunogenicity and longer circulation durability due to the presence of red-cell membrane proteins,[135] or precision delivery owing to the homologous targeting ability of cancer cells. Subsequently, the hybrid membranes formed by erythrocyte and specific cancer cell membranes will be discussed.

Erythrocyte and Gastric Cancer Cell sMembrane

Long et al[126] prepared pH-responsive liposomes containing apatinib (AP) and CBG, followed by coating them with hybrid membranes (R/C) to construct nanocomposites (LP-R/C@AC) for combined treatment of gastric cancer. The R/C can make the nanocomposite to exhibit the dual ability of immune escape and tumor targeting, and to prolong the half-life of the single drug. At the optimal ratio of AP to CBG, the dosage was reduced by 42.33% (AP) and 23.82% (CBG), respectively, compared to the IC_{50} value of single drug. The killing effect on HGC-27 cells was 3.48 times and 1.84 times higher than that of the corresponding concentration of AP or CBG single drug, respectively. LP-R/C@AC exhibited the highest TIR of 86.78% in vivo, surpassing that of single drugs and uncoated liposomes. Furthermore, immunofluorescence results for PD-L1 and MMP-9 demonstrated the capacity of LP-R/C@AC to inhibit tumor invasion and metastasis, thereby corroborating its excellent antitumor effects.

Erythrocyte and Colon Cancer Cell Membrane

Luo et al[127] developed a novel approach for treating colorectal cancer (CRC) by utilizing CBG-loaded Prussian blue NPs (PC@M NPs), which were coated with hybrid membranes and combined with photothermal therapy (PTT). In vivo half-

life of PC^{Ce6}@M NPs was found to be 4.338 times longer than that of Ce6 (1.983 h vs 0.4571 h). Compared to free CBG, PC@M NPs demonstrated an enhanced tumor inhibition rate in vivo to 57.87%, and when combined with PTT, the TIR could reach as high as 84.57%. Additionally, studies on gut microbiota have shown that PC@M NPs + PTT could inhibit the growth of colorectal cancer by regulating gut microbiota, suggesting that we should pay attention to the effect of drug use on its internal environment from the microbial level.

Erythrocyte and Triple Negative Breast Cancer Cell Membrane

Zeng et al[128] synthesized peroxidase-active CeO_2 NPs (Ce NPs) that were modified by PAA for the purpose of loading CBG and Chlorin e6 (Ce6), with a hybrid membrane to form a nanocomposite (CPCCM), which was combined with chemotherapy-PDT to treat triple-negative breast cancer (TNBC). The coated hybrid membrane retained the characteristic function of the original cells, possessing homologous targeting ability and facilitating long blood circulation. In vivo biodistribution showed that the accumulation of CPCCM in tumors increased by 23.7% compared with the uncoated NPs. In addition, the TIR was only 77.5% in the CPCC + PDT group, but up to 85.5% in the CPCCM + PDT group. In the blood routine examination, without membrane coated leukocyte levels of each treatment group was obviously increased after the biomimetic membrane coated can effectively reduce the immune response. (Figure 5). Long et al[129] prepared biomimetic Prussian blue nanocomposites (CS-1@PB[HM] NPs) loaded with CBG used to treat TNBC. The fluorescence signal of the hybrid membrane-coated NPs was found to be decreased by more than 50% in RAW264.7 cells, suggesting that membrane camouflage can significantly enhance the immune escape ability. The membrane-modified NPs had a longer half-life (1.2 h vs 0.41 h) and stronger tumor targeting ability (fluorescence signal increased by 2.35 times). In the mouse model, CS-1@PB[HM] NPs showed good tumor inhibition (72.8%). When combined with laser irradiation, the tumor inhibition rate was further increased by 10.6%. Fan et al[130] developed two delivery systems encapsulated by

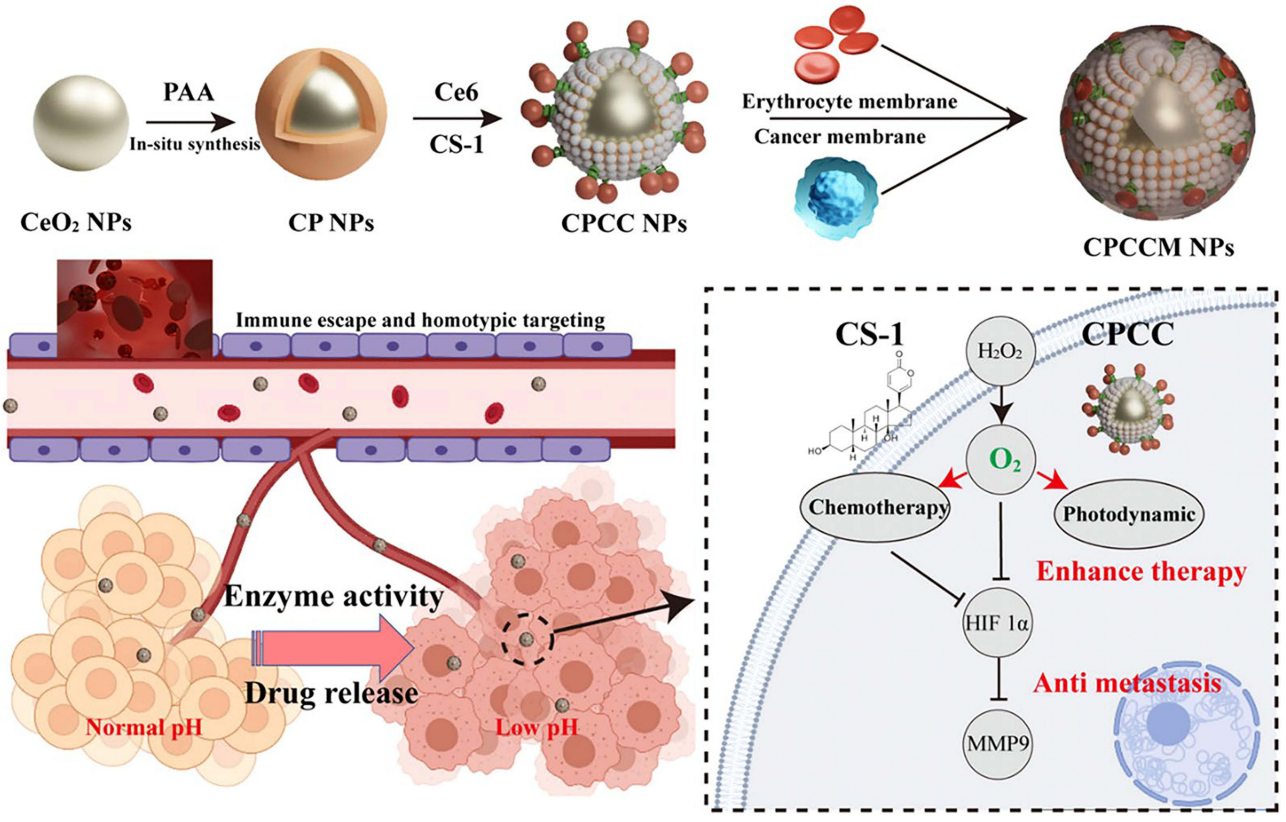

Figure 5 Schematic diagram of the designed strategy for the combined therapy of CPCCM NPs. Reproduced from Zeng Z, Wang Z, Chen S et al. Bio-nanocomplexes with autonomous O_2 generation efficiently inhibit triple negative breast cancer through enhanced chemo-PDT. *Journal of Nanobiotechnology.* 2022;20(1):500. Creative Commons.[128]

hybrid membranes, which were used to deliver capsaicin (HM-PLGA@Cap NPs) and co-loaded GBF and Ce6 (HM-PLGA@GC&CS-6 NPs), respectively, to inhibit the growth of TNBC by sequential administration. In MDA-MB-231 or 4T1 Luc tumor orthotopic model with high therapeutic efficiency can be attributed to the high tumor targeting and penetration ability of HM-PLGA@GC&CS-6 NPs assisted by HM-PLGA@Cap NPs.

Erythrocyte and Cervical Cancer Cell Membrane

Xiao et al[131] prepared a biomimetic nanodelivery system loaded with GBF and indomethacin on a hybrid membrane (PCDI@M). This nanodelivery system exhibited a stronger red fluorescence signal than the uncoated group, indicating that it could obtain homologous targeting ability through the cell membrane and significantly enhance the cellular uptake ability. Furthermore, pharmacokinetics in vivo demonstrated that the blood half-life was increased by nearly 1.5 times compared to bare leak NPs. In vitro imaging revealed that the majority of the drug accumulated in tumor tissues, thereby further substantiating the advantage of bionic nanoparticle delivery systems.

Stimuli-Responsive Targeted Drug Delivery Systems

Nanomedicine has been extensively studied in drug delivery systems with the aim of improving efficacy and reducing toxicity by either enhancing the EPR effect or active targeting.[136] However, in recent years, stimuli-responsive nano delivery systems have attracted much attention due to their ability to provide more controlled drug release and precise delivery. Stimuli-responsive TDDS are mainly based on the ability of nanocarrier materials to undergo structural changes in response to certain stimuli, including chemical bond breaking and molecular structure changes, so as to achieve controlled drug delivery.[137] Depending on the source of biological stimuli, stimuli-responsive TDDS can also be divided into endogenous and exogenous responses. Endogenous stimuli are typically influenced by the TME, including low pH, high glutathione (GSH) and reactive oxygen species (ROS) levels, while exogenous stimuli are primarily affected by external factors such as temperature, magnetic field and light irradiation. These factors collectively enable the realization of stimuli-responsive TDDS, facilitating controlled drug release and enhanced drug accumulation at tumor sites, while concurrently reducing the toxic side effects on normal tissues.[138,139]

Thermal Response

Thermally responsive NPs are among the most common types of stimuli-responsive systems for controlled drug release. By exploiting temperature changes, these systems enhance the precision and efficacy of drug delivery. Poly (N-isopropyl acrylamide) (PNIPAM) is particularly promising as it undergoes a sol-gel transition under physiological conditions, allowing for minimal invasive delivery of the drug and minimizing side effects.[137] A study utilized PNIPAM and PLA NPs loaded with BU and modified with EGFR antibodies to form dual-targeted immunomicelles (DTIs-BF). The heat-sensitive properties of PNIPAM render the immunomicelles temperature-sensitive, facilitating drug delivery to tumor tissues, which typically have higher temperatures than surrounding normal tissues. SMMC-7721 cells at 40 °C exhibited lower viability compared to those at 37 °C, highlighting the thermally responsive nature of the DTIs-BF. Additionally, the EGFR antibody modification enhanced the accumulation of BU at the tumor site, leading to improved anticancer effects.[140]

Photoresponse

Light-responsive targeted delivery systems can be classified into photothermal therapy (PTT) and photodynamic therapy (PDT), each exploiting different mechanisms to enhance drug delivery and therapeutic efficacy. PTT is a non-invasive cancer treatment that utilizes light to raise the local temperature at the tumor site, enhancing drug penetration and release with minimal systemic side effects.[141] He et al[142] prepared a composite hydrogel (BP-bufalin@SH) co-loaded with black phosphorus nanosheets (BPNSs) and BU, achieving photothermal chemotherapy. BPNSs exhibit high photothermal conversion efficiency, making the hydrogel's temperature under near-infrared irradiation dependent on both time and BPNS concentration. This leads to a significant increase in BU release. In HepG2 mouse models, BP-bufalin@SH demonstrated slow drug release and, when subjected to laser irradiation, facilitated significant antitumor effects through enhanced bufalin release. PDT relies on the generation of ROS through photosensitizers (PSs) activated by light to induce

cellular toxicity and tumor ablation. However, the hypoxic TME can limit PDT effectiveness.[143] Yuan et al[144] addressed this by preparing the nano composites of PSs mTHPC and BU (T-B@NP) for combined chemo-PDT therapy. The singlet oxygen quantum yield of T-B@NP was only slightly lower than free mTHPC (0.36 vs 0.43), and its good ROS generation ability provides an important basis for PDT research. T-B@NP + PDT significantly inhibited the proliferation of HCT116 cells (IC_{50} = 0.25 μg/mL), and in the CRC model, showed superior antitumor effect (TIR: 84.25%) than other groups. In addition, the ROS-induced structural disruption of the nanocomposites facilitated BU release, providing antitumor effects and alleviating hypoxia, thus overcoming PDT limitations and achieving a synergistic therapeutic outcome.

Photomagnetic Response

Magnetic NPs have now become an effective delivery tool, utilizing an external magnetic field to direct and localize these particles within cancer cells. This magnetic guidance enhances the accumulation of NPs in tumor sites and allows for controlled drug release and precise localization when combined with light and heat.[145] Hu[146] used superparamagnetism Fe_3O_4 NPs as the carrier to prepare photomagnetic dual-sensitive BU liposomes (BF-Fe_3O_4-L). Application of a magnetic field increased drug uptake by 1.6 times compared to conditions without the magnetic field. In vivo studies demonstrated that the treatment group achieved a TIR of 91.0% and an 81.5% reduction in pulmonary metastasis incidence compared to the blank control group. These findings indicated that BF-Fe_3O_4-L can effectively inhibit breast cancer growth and reduce lung metastasis.

Thermal and Redox Response

Redox-sensitive particles respond to high redox potentials by disrupting their linker, leading to the rapid drug release and subsequent disintegration of the nanocarrier. According to the potential difference between tumor cells and normal cells to achieve precise delivery and fast drug release. The concentration of GSH in tumor cells is 100 to 1000 times and 100 times higher than in blood and normal tissues, respectively, creating a large gradient that ensure the sensitivity of the redox-response drug delivery system.[147] However, relying solely on a redox response lacks specificity. Therefore, Wang et al[148] developed novel thermal and redox-responsive micelles using Pluronic F127 triblock copolymer for BU delivery. The average diameter of the cross-linked micelles was significantly greater at 4 °C than at 37 °C, allowing for high EE (79.6 ± 1.2) % and DL (2.9 ± 0.2) %, at 4 °C, which dropped to EE (21.5 ± 1.3) % and DL (1.9 ± 0.2) %, at 37 °C. Additionally, In the presence of 10 mM GSH at pH = 7.4, after 48h, BU release reached (69 ± 1) %, compared towithout GSH [the release rate of BU was (33 ± 1) %]. The cross-linked micelles significantly enhanced the apoptosis-inducing ability, compared to free BU and non-crosslinked micelles. Furthermore, in vivo antitumor studies showed that the drug-loaded cross-linked micelles extended the survival period to over 36 days, showing significant therapeutic potential.

pH Response

Cancer cells exhibit polarized extracellular acidity, a distinctive metabolic feature resulting from aerobic glycolysis, which is characterized by severe surface acidity. This pH polarization makes it feasible to exploit the lower pH (<5.5) of tumor tissues to develop pH-responsive targeted drug delivery systems (TDDS), in contrast to the neutral pH (~7.4) of normal tissues.[149] Chen et al[150] developed a pH responsive TDDS co-loaded apatinib (Apa) and GBF using Prussia NPs (HA-Apa-Lip@PB-CS-6 NPs) for the treatment of metastatic gastric cancer. This system leverages the pH-sensitive lipid DSPE-PEOz to enhance drug release under acidic conditions, with GBF release significantly increased at pH = 5.2 compared to pH = 7.4 (64.4% vs 17.0%). Compared with the free of Apa and GBF, HA-Apa-Lip@PB-CS-6 NPs showed efficient accumulation at the tumor site, controlled drug release and remarkably low cardiotoxicity, highlighting the potential for enhanced therapeutic efficacy and safety in cancer treatment.

pH and Redox Response

Taking advantage of low pH and high GSH levels characteristic of the TME, Zeng et al[151] developed a novel drug delivery system utilizing GSH-sensitive organic ligands to construct a pH-sensitive and redox-responsive folic acid-modified metal-organic framework (MOF) loaded with BU NPs (FA-MOF/Buf). In vitro release experiments revealed that the release of BU reached 62.8% at pH = 7.4 and 78.8% at pH = 6.5, which were 1.8-fold and 1.4-fold higher than

that in the absence of GSH, respectively. Moreover, under conditions of pH = 5.5 with 10mM GSH, the release rate of BU over 48 h reached 81.2%, indicating that FA-MOF/Buf achieved optimal drug release at the tumor site. Acidic conditions and redox responsiveness facilitate the accelerated dissociation of the MOF structure, thereby enhancing bufalin release and maximizing its therapeutic effect. In the TME, the NPs can be rapidly degraded, resulting in increased cellular uptake and enhanced cytotoxic effects.

pH and Photothermal Response

The multiple response to pH and photothermal is a commonly employed strategy in TDDS. Leveraging the photothermal properties of nanocapsules and the low pH of the TME, these nanosystems can enhance drug efficacy, control drug release through photothermal ablation, increase drug release at low pH levels and improve drug targeting. Li et al[152] investigated folate-modified dopamine-loaded CBG NPs with pH and photothermal response. Due to the pH sensitivity of the PDA nanocarriers, the drug release rate was higher at pH = 5.0 compared to at pH = 7.4 (24 h, pH = 5.0/7.4; no irradiation, 53%/24%; irradiation, 74%/33%). The nanodrugs showed an increase in the drug release with temperature at pH = 5.0 under 808 nm laser irradiation, indicating that PTT could improve the efficacy of CBG-loaded PDA NPs in the treatment of lung cancer. Furthermore, near infrared laser PDA nanodrugs effectively inhibited tumor growth (TIR: free CBG/ CBG-PDA NPs/CBG-PDA NPs + L: 29%/48%/67%). The temperature in the PDA nanodrug treatment group reached 42.7 °C after laser irradiation, meeting the therapeutic range for phototherapy (42–45 °C), whereas the temperature in the free CBG treatment group was only 34.9 °C. The experimental results showed that the near infrared laser PDA nanodrugs effectively suppress tumor development through combined low pH stimulation and photothermal response (Figure 6).

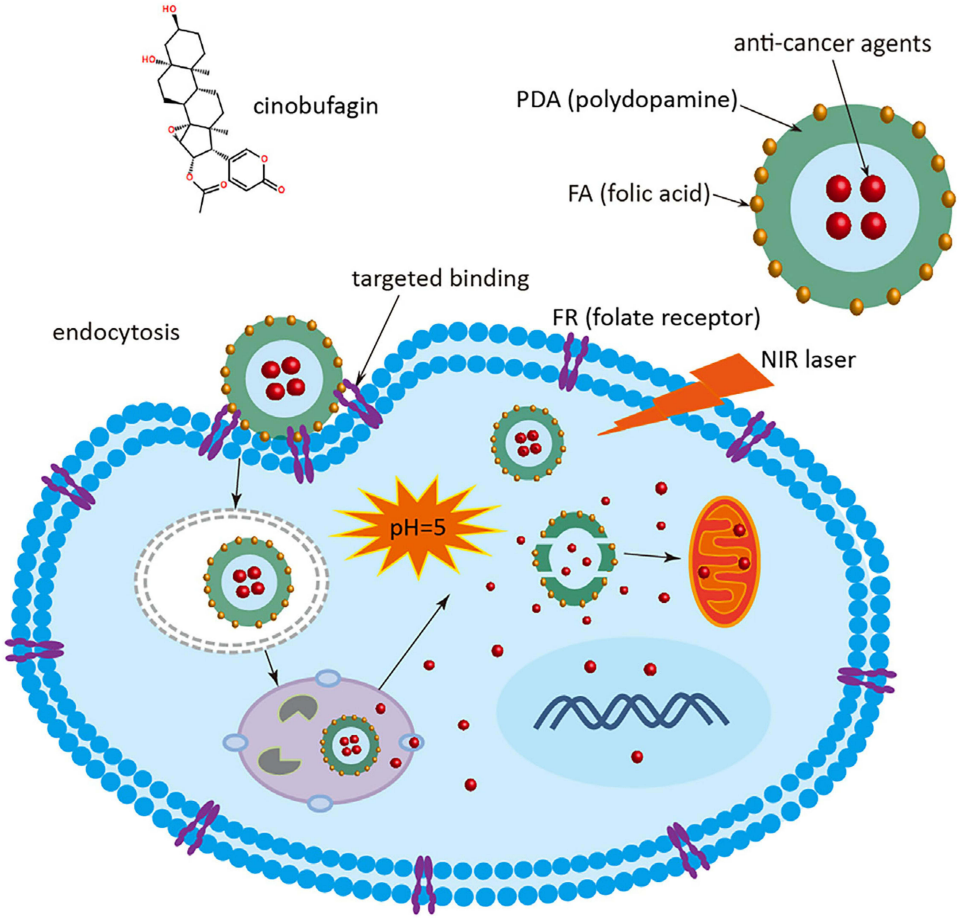

Figure 6 Schematic diagram of Cino nanomedicine with targeted delivery and smart response. Cino, cinobufagin; PDA, polydopamine; FA, folic acid; FR, folate receptor; NIR, near infrared. Reproduced from Li J, Zhang Z, Deng H and Zheng Z. Cinobufagin-Loaded and Folic Acid-Modified Polydopamine Nanomedicine Combined with Photothermal Therapy for the Treatment of Lung Cancer. *Front. Chem*. 2021,9:637754. Creative Commons.[152]

Conclusion and Prospectives

Traditional Chinese medicine (TCM) has been pivotal in the management and treatment of various diseases. TS and TV, as traditional Chinese medicine, have been widely used in the treatment of various cancers. Research shows that 9 bufogenins can be identified from the TS/TV, including those mentioned in this article such as BU, CBF, CBG, ABG, RBG and GBF.[153] Although they exhibit significant antitumor effects, their structure is similar to cardiac glycosides leading to toxic. Additionally, their rapid metabolism, poor water solubility, and short half-life limit their clinical application.[154,155] Therefore, to address these challenges, researchers are developing various drug delivery systems to enhance their therapeutic efficacy. Recently, a wide range of research has focused on TDDS for TS/TV and their active ingredients. This paper summarizes these developments, including strategies based on EPR effect, receptor-mediated, homologous targeted and endogenous or exogenous stimuli responses. BU, CBG, CBF, RBG, ABG and GBF were developed within various TDDS, demonstrating superior tumor targeting, enhanced antitumor effects, and reduced toxic side effects compared to the free drugs. This indicates that the advancement of TDDS could expand the clinical application of TS/TV.

Utilizing passive, active and stimuli-responsive TDDS for TS/TV and their active ingredients can improve the drug solubility in water, extend the functional duration of the drug in the body, enhance therapeutic efficacy and reduce the toxicity to major organs. Passive targeting leverages the EPR effect to enhance the antitumor activity.[156] Polymeric micelles, emulsions, microspheres, liposomes and NPs loaded with active ingredients can address issues like poor water solubility, rapid metabolism, low absorption and specific toxic side effects in vivo. Additionally, passive TDDS also have the advantages of simple preparation, low cost, and low development difficulty, which are convenient for clinical application and transformation.[157] However, the tumor penetration of nanomedicine can be significantly affected by physicochemical properties such as size, surface chemistry, and shape.[158] Therefore, rational design and modification, such as PEG-modified liposomes, can enhance the water solubility of liposomes, reduce the possibility of their phagocytosis, prolong their retention time in vivo, and improve tumor penetration by employing cell-penetrating peptides such as TAT peptide. Moreover, the EPR effect can exhibit tumor heterogeneity, its efficacy may vary among different tumors or even within the same tumor, which will lead to inconsistent drug accumulation in vivo and reduced therapeutic effect, and the efficiency of passive targeting depends on the leaky vasculature of the tumor. Additionally, healthy tissues or inflamed areas may also exhibit vascular leakage, potentially leading to toxicity and off-target effects on non-cancerous tissues, reducing the selectivity of passive targeting.[159] Thus, further exploration of the EPR mechanism or pre-treatment of tumor tissue before administration is necessary to enhance passive targeting and improve drug efficacy.

Active targeting ligands used on nanocarriers commonly include small molecules, peptides, proteins, and antibodies.[160] Surface modification with these ligands allows receptor-mediated endocytosis to achieve more precise and maximal accumulation at the tumor site compared to EPR effect of passive targeting.[161] However, their delivery efficiency depends on selecting effective receptors, appropriate drug carriers, and proper passivation of carrier-ligand complexes. Therefore, ligand-modified NPs should be designed to target receptors that are expressed at high or exclusive levels in cancer cells, and the purification of non-conjugated ligands is also of importance, as their presence can reduce the efficacy of targeting. Additionally, the surface characteristics of drug carriers must be managed to prevent protein corona formation, which can lead to rapid clearance and ineffective treatment in vivo.[162] Biomimetic nano-systems, which utilize natural cell membrane-coated NPs, offer immune evasion, precise targeting and excellent biocompatibility. For instance, erythrocyte membrane can prolong the circulation time in vivo, platelet membranes can target wounds, bacteria and tumor cells and cancer cell membrane can achieve tumor homologous targeting. Hence, biomimetic NPs hold broad therapeutic potential.[163] Biomimetic nano-delivery systems can lead to immune system disorders and inflammation if the membrane surface is over-designed. The variability in membrane proteins also complicates reproducibility between batches. Thus, controlling the type and amount of ligands on the membrane surface is crucial for enhancing biocompatibility and long-term biosafety, and developing consistent therapeutic mechanisms for clinical translation.[164]

Stimuli-responsive delivery systems, also known as physicochemical targeted delivery, enable drug effects at specific sites through physical or chemical methods. Stimuli signals are categorized as endogenous (eg, ROS, pH, and redox

responses) and exogenous (eg, temperature, laser, and magnetic fields). Compared to the passive and active TDDS, stimuli-responsive nanodelivery systems are characterized by their ability to exploit the specificity of the TME for enhancing drug targeting accuracy and controlling drug release through endogenous or exogenous stimuli, thereby improving drug efficacy and reducing adverse reactions.[165] Although stimuli-responsive drug delivery systems can successfully overcome physiological barrier of the tumor site, the particle size and surface charge distribution of nanocarriers play a critical role in cellular responses in vivo. Therefore, it is crucial to monitor the stimulation sensitivity of nanocarriers at the target site to prevent off-target effects arising from inaccurate stimulation distribution. Consequently, it is of paramount importance to monitor the stimulation sensitivity of nanocellulators at the target site in order to prevent off-target effects resulting from an inaccurate distribution of stimulation.[166] For example, low pH is a common stimulus, but it may also be present in some healthy tissues, so the pH to which the nanomaterials respond is crucial for controlled release at the target site. Additionally, the complexity and heterogeneity of the tumor environment result in poor sensitivity to a single stimulus, leading to ineffective positioning capability. Therefore, developing multiple stimuli-responsive compounds and further exploring TDDS at both academic and pharmaceutical levels are essential.[167]

Studies have found that different delivery methods significantly impact delivery efficiency. Currently, cinobufacini capsules and tablets in clinical use are administered orally, but this method is limited by poor water solubility, low permeability, instability, rapid metabolic elimination in the intestine and liver.[168] Cinobufacini and TV injections can overcome the limitations of oral administration via intramuscular or intravenous injection, but they exhibit rapid blood clearance, toxic side effects at high concentrations, and weak tumor targeting, resulting in suboptimal effects. Numerous studies have demonstrated that TS/TV and active ingredients of TDDS were designed by intravenous administration delivery, which allowed them to improve water solubility, enhance stability, prolong blood circulation time, reduce internal clearance, and have good tumor targeting, thereby enhancing their therapeutic efficacy. However, in the past few decades, despite significant advances in TDDS, as of 2020, only 10 nanoparticle-based nanomedicines have been approved for clinical cancer treatment by the Food and Drug Administration and the European Medicines Agency. Of the drugs that have entered Phase III clinical trials, only 14% have successfully demonstrated efficacy.[169] Additionally, studies and analyses have shown that the mean and median delivery efficiency after intravenous administration is only 2.24% and 0.76% in 24 h, which is quite low and undoubtedly increases the difficulty of clinical translation.[170] In comparison to intravenous drug delivery, nano-local drug delivery systems are regarded as a promising approach to enhance drug concentration at the target site. This is achieved by confining the drug to the local disease site, thereby reducing the toxicity and preventing drug entry into non-target sites, ultimately leads to improved efficacy.[171] For instance, the injectable hydrogel (BP-bufalin@SH) prepared by He et al[142] demonstrated better antitumor effect, and the Dox nano gel prepared by Dosta et al[172] for local delivery can bypass the blood-brain barrier to treat glioblastoma, showing delayed tumor growth and overall improved survival. Furthermore, local injection is considered a promising method to combat tumor recurrence post-surgery.[173] Although, this delivery method has been gradually studied, research on TS/TV remains limited. In the future, further explored is required, especially for tumors with superficial skin layer, in order to demonstrate more surprising therapeutic potential.[174]

Nevertheless, the potential of nano-delivery systems in cancer treatment cannot be underestimated, with a significant increase in the number of FDA-approved and clinical trials utilizing NPs over the past few years.[175] Concurrent advancements in artificial intelligence are providing invaluable support for constructing predictive models of nano-biological interactions, assessing hierarchical targeting efficiency, and enhancing the safety and therapeutic efficacy of nanomedicines.[176] The therapeutic efficacy of the antitumor active ingredients of TS and TV including BU, CBG, CBF, RBG, ABG and GBF, has been well-documented. Researchers are increasingly exploring TDDS for these active ingredients to achieve higher antitumor activity with minimal toxic side effects. However, the clinical translation of these systems faces significant obstacles. Many experiments remain at the animal level, and challenges such as improper clinical trial design, insufficient sample sizes, inadequate patient selection persist, the regulatory challenges in the market and the fierce competition of therapeutic drugs. To facilitate successful clinical translation, it is crucial to develop rational design strategies, select representative preclinical models, design precise clinical trials, establish an effective regulatory framework, and secure financial support.[177] With ongoing advancements in nanomedicine, TDDS are poised to inject new vitality into cancer treatment, potentially becoming a formidable force in future therapeutic strategies.

Author Contributions

All authors made a significant contribution to the work reported, whether that is in the conception, study design, execution, acquisition of data, analysis and interpretation, or in all these areas; took part in drafting, revising or critically reviewing the article; gave final approval of the version to be published; have agreed on the journal to which the article has been submitted; and agree to be accountable for all aspects of the work.

Funding

This research was supported by grants from National Natural Science Foundation of China (grant No. 82204935) and Innovation Team of Shaanxi University of Chinese Medicine (NO. 2019-YL11).

Disclosure

The authors report no conflicts of interest in this work.

References

1. Jassim A, Rahrmann EP, Simons BD, Gilbertson RJ. Cancers make their own luck: theories of cancer origins. *Nat Rev Cancer*. 2023;23(10):710–724. doi:10.1038/s41568-023-00602-5
2. Bray F, et al. Global cancer statistics 2022: GLOBOCAN estimates of incidence and mortality worldwide for 36 cancers in 185 countries. *Ca a Cancer J Clinicians*. 2024;74:229–263. doi:10.3322/caac.21834
3. Siegel RL, Giaquinto AN, Jemal A. Cancer statistics, 2024. *Ca a Cancer J Clinicians*. 2024;74(1):12–49. doi:10.3322/caac.21820
4. Brown JS, Amend SR, Austin RH, et al. Updating the Definition of Cancer. *Mol Cancer Res*. 2023;21(11):1142–1147. doi:10.1158/1541-7786.Mcr-23-0411
5. Yang CY, Shiranthika C, Wang CY, Chen KW, Sumathipala S. Reinforcement learning strategies in cancer chemotherapy treatments: a review. *Comput. Methods Programs Biomed.* 2023;229:107280. doi:10.1016/j.cmpb.2022.107280
6. Lepeltier E, Rijo P, Rizzolio F, et al. Nanomedicine to target multidrug resistant tumors. *Drug Resist Updates*. 2020;52:100704. doi:10.1016/j.drup.2020.100704
7. He S, Gou X, Zhang S, et al. Nanodelivery Systems as a Novel Strategy to Overcome Treatment Failure of Cancer. *Small Methods*. 2023;8(1):e2301127. doi:10.1002/smtd.202301127
8. Wang Y, et al. Application of immune checkpoint targets in the anti-tumor novel drugs and traditional Chinese medicine development. *Acta Pharmaceutica Sinica B*. 2021;11(10):2957–2972. doi:10.1016/j.apsb.2021.03.004
9. Liu Y, Fang C, Luo J, et al. Traditional Chinese Medicine for Cancer Treatment. *Am J Chin Med*. 2024;52(03):583–604. doi:10.1142/s0192415x24500253
10. Zhan X, Wu H, Wu H, et al. Metabolites from Bufo gargarizans (Cantor, 1842): a review of traditional uses, pharmacological activity, toxicity and quality control. *J Ethnopharmacol*. 2020;246:112178. doi:10.1016/j.jep.2019.112178
11. Liu Q, Lei Z. Adverse reactions and rational use of cinobufacini injection. *Chinese Traditional Patent Med*. 2012;34:1409–1411.
12. Qi J, Tan CK, Hashimi SM, et al. Toad glandular secretions and skin extractions as anti-inflammatory and anticancer agents. *Evid Based Complement Alternat Med*. 2014;2014:312684. doi:10.1155/2014/312684
13. Sun Y, Bi J, Zhang L, Ye B. Ultrasound-assisted extraction of three bufadienolides from Chinese medicine ChanSu. *Ultrason Sonochem*. 2012;19(6):1150–1154. doi:10.1016/j.ultsonch.2012.03.003
14. Wu JH, Cao YT, Pan HY, Wang LH. Identification of Antitumor Constituents in Toad Venom by Spectrum-Effect Relationship Analysis and Investigation on Its Pharmacologic Mechanism. *Molecules*. 2020;25(18):4269. doi:10.3390/molecules25184269
15. Zuo Q, Xu DQ, Yue SJ, Fu RJ, Tang YP. Chemical Composition, Pharmacological Effects and Clinical Applications of Cinobufacini. *Chin J Integr Med*. 2024;30(4):366–378. doi:10.1007/s11655-024-3708-6
16. Sampath V, Horesh N, Sasi B, et al. Synthesis and Biological Evaluation of Novel Bufalin Derivatives. *Int J Mol Sci*. 2022;23(7):4007. doi:10.3390/ijms23074007
17. Burlacu E, Tanase C. Anticancer Potential of Natural Bark Products-A Review. *Plants*. 2021;10(9):1895. doi:10.3390/plants10091895
18. Huang L, Huang X-H, Yang X, et al. Novel nano-drug delivery system for natural products and their application. *Pharmacol Res*. 2024;201:107100. doi:10.1016/j.phrs.2024.107100
19. Li J, Wang Q, Xia G, et al. Recent Advances in Targeted Drug Delivery Strategy for Enhancing Oncotherapy. *Pharmaceutics*. 2023;15(9):2233. doi:10.3390/pharmaceutics15092233
20. Dutta B, Barick KC, Hassan PA. Recent advances in active targeting of nanomaterials for anticancer drug delivery. *Adv. Colloid Interface Sci.* 2021;296:102509. doi:10.1016/j.cis.2021.102509
21. Li J, Zeng H, Li L, et al. Advanced Generation Therapeutics: biomimetic Nanodelivery System for Tumor Immunotherapy. *ACS Nano*. 2023;17(24):24593–24618. doi:10.1021/acsnano.3c10212
22. Kang C, Wang J, Li R, et al. Smart Targeted Delivery Systems for Enhancing Antitumor Therapy of Active Ingredients in Traditional Chinese Medicine. *Molecules*. 2023;28(16):5955. doi:10.3390/molecules28165955
23. Huang M, Zhai B-T, Fan Y, et al. Targeted Drug Delivery Systems for Curcumin in Breast Cancer Therapy. *Int j Nanomed*. 2023;18:4275–4311. doi:10.2147/ijn.S410688
24. Jia J, Li J, Zheng Q, Li D. A research update on the antitumor effects of active components of Chinese medicine ChanSu. *Front Oncol*. 2022;12:1014637. doi:10.3389/fonc.2022.1014637

25. Soumoy L, Ghanem GE, Saussez S, Journe F. Bufalin for an innovative therapeutic approach against cancer. *Pharmacol Res*. 2022;184:106442. doi:10.1016/j.phrs.2022.106442
26. Shao H, Li B, Li H, et al. Novel Strategies for Solubility and Bioavailability Enhancement of Bufadienolides. *Molecules*. 2021;27(1):51. doi:10.3390/molecules27010051
27. Behera A, Padhi S. Passive and active targeting strategies for the delivery of the camptothecin anticancer drug: a review. *Environ. Chem. Lett.* 2020;18(5):1557–1567. doi:10.1007/s10311-020-01022-9
28. Chen Z, Kumar Kankala R, Long L, Xie S, Chen A, Zou L. Current understanding of passive and active targeting nanomedicines to enhance tumor accumulation. *Coord. Chem. Rev.* 2023;481:215051. doi:10.1016/j.ccr.2023.215051
29. Caro C, Avasthi A, Paez-Muñoz JM, Pernia Leal M, García-Martín ML. Passive targeting of high-grade gliomas via the EPR effect: a closed path for metallic nanoparticles? *Biomater. Sci.* 2021;9(23):7984. doi:10.1039/d1bm01398j
30. Qi QR, Tian H, Yue BS, Zhai BT, Zhao F. Research Progress of SN38 Drug Delivery System in Cancer Treatment. *Int j Nanomed*. 2024;19:945–964. doi:10.2147/ijn.S435407
31. Xiao P. *Preparation and Evaluation of Mesoporous Silica Nanoparticles Loaded with Effective. Master's Thesis*. Guangzhou University of Chinese Medicine; 2022. doi:10.27044/d.cnki.ggzzu.2021.000563
32. Xu H, et al. Quality evaluation of resibufogenin-loaded PLGA-TPGS nanoparticles. *Chin J Hospital Pharm*. 2017;37:809–813. doi:10.13286/j.cnki.chinhosppharmacyj.2017.09.06
33. Xu H, et al. Prescription selection and stability evaluation of resibufogenin-loaded PLGA-TPGS nanoparticles. *Chin J Hospital Pharm*. 2017;37:1017–1022. doi:10.13286/j.cnki.chinhosppharmacyj.2017.11.04
34. Xu H, et al. Hepatic targeting properties of Resibufogenin-loaded PLGA-TPGS nanoparticles in mice. *Chin J Hospital Pharm*. 2017;37:590–595+612. doi:10.13286/j.cnki.chinhosppharmacyj.2017.07.06
35. Xu H, et al. Study on the in vitro Cell Uptake and Toxicity of Resibufogenin-loaded PLGA-TPGS Nanoparticles. *China Pharm*. 2017;28:2252–2255. doi:10.6039/j.issn.1001-0408.2017.16.25
36. Xu H, et al. Study the inhibition of Resibufogenin-loaded PLGA-TPGS Nanoparticles on the hepatocarcinoma ectopic transplantation tumor-bearing mice. *Chin J Hospital Pharm*. 2017;37:1388–1392. doi:10.13286/j.cnki.chinhosppharmacyj.2017.14.15
37. Chen M. Preparation and evaluation of bufalin coated PBCA nanoparticles. *Chin Traditional Herbal Drugs*. 2015;46:1296–1301. doi:10.7501/j.issn.0253-2670.2015.09.008
38. Hu Q, Liang B, Sun Y, et al. Preparation of bufalin-loaded pluronic polyetherimide nanoparticles, cellular uptake, distribution, and effect on colorectal cancer. *Int j Nanomed*. 2014;9:4035–4041. doi:10.2147/ijn.S64708
39. Hu M, et al. Bufalin-loaded Pluronic-PEI nanoparticles inhibits the invasion and metastasis of colorectal cancer via miRNA-497 mediated IGF1-R-PI3K-Akt signaling pathway. *Shanghai J Traditional Chin Med*. 2017;51:89–96. doi:10.16305/j.1007-1334.2017.10.025
40. Yang Y, et al. Pharmacokinetics of lyophilization of toad venom-loaded solid lipid nanoparticles. *Chinese Traditional Patent Med*. 2006;28:787–790.
41. Yang Y, et al. Freeze-drying and characteristics of Chansu-loaded solid lipid nanoparticles. *Central South Pharm*. 2006;4:163–166.
42. Yang Y, Feng J-F, Zhang H, et al. Preparation process of toad venom solid lipid nanoparticles was optimized by central composite design-response surface method. *China J Chinese Materia Medica*. 2006;31(8):650–653.
43. Yang Y, et al. Distribution of Lyophilized SLN Loaded with Venenum Bufonis in Mice. *Chin J Pharm*. 2007;38:354–356+371.
44. Zhang L, et al. Quality Evaluation of Solid Lipid Nanoparticle of the Skin Extract of Bufobufo gargarizans. *Chin. Pharm*. 2016:27:1400–1403. doi:10.6039/j.issn.1001-0408.2016.10.31
45. Zhang L, et al. Study on the freeze-drying technology of solid lipid nanoparticles from toad skin extract. *Anhui Med Pharm J*. 2020;24:78–82.
46. Su Y-H, Zhang J-G, Shen J, et al. PREPARATION OF CINOBUFAGIN-LOADED BOVINE SERUM ALBUMIN NANOPARTICLES FOR HEPATOCARCINOMA THERAPY. *Nano*. 2009;04(01):47–54. doi:10.1142/s1793292009001472
47. Zhang H, Huang N, Yang G, Lin Q, Su Y. Bufalin-loaded bovine serum albumin nanoparticles demonstrated improved anti-tumor activity against hepatocellular carcinoma: preparation, characterization, pharmacokinetics and tissue distribution. *Oncotarget*. 2017;8(38):63311–63323. doi:10.18632/oncotarget.18800
48. Long L, Zhong W, Guo L, Ji J, Nie H. Effect of Bufalin-PLGA Microspheres in the Alleviation of Neuropathic Pain via the CCI Model. *Front Pharmacol*. 2022;13. doi:10.3389/fphar.2022.910885
49. Chen X, et al. Preparation of polylactic acid microspheres containing lactones from Venenum Bufonis, its slow-release characteristics and therapeutic effects on mycoplasmal pneumonia of swine. *Chin J Vet Sci*. 2015;35:2014–2020. doi:10.16303/j.cnki.1005-4545.2015.12.24
50. Jing J, Tupally KR, Kokil GR, et al. Development of a hybrid peptide dendrimer micellar carrier system and its application in the reformulation of a hydrophobic therapeutic agent derived from traditional Chinese medicine. *RSC Adv*. 2019;9(5):2458–2463. doi:10.1039/c8ra09606f
51. Liu Q, et al. Study on Preparation of Polymer Micelle of Toad Venom. *J Liaon Univ TCM*. 2018;20:81–85. doi:10.13194/j.issn.1673-842x.2018.07.022
52. Yuan X, Xie Q, Su K, et al. Systemic delivery of the anticancer agent arenobufagin using polymeric nanomicelles. *Int j Nanomed*. 2017;12:4981–4989. doi:10.2147/ijn.s139128
53. Shen L, et al. Bufotenines-loaded liposome exerts anti-inflammatory, analgesic effects and reduce gastrointestinal toxicity through altering lipid and bufotenines metabolism. *Biomed Pharmacothe*. 2022;153:113492. doi:10.1016/j.biopha.2022.113492
54. Gao L, et al. Surfactant Assisted Rapid-Release Liposomal Strategies Enhance the Antitumor Efficiency of Bufalin Derivative and Reduce Cardiotoxicity. *Int j Nanomed*. 2021;16:3581–3598. doi:10.2147/ijn.S313153
55. Yuan J, Zhou X, Cao W, et al. Improved Antitumor Efficacy and Pharmacokinetics of Bufalin via PEGylated Liposomes. *Nanoscale Res Lett*. 2017;12(1):585. doi:10.1186/s11671-017-2346-8
56. Yuan J, et al. Bufalin-Loaded PEGylated Liposomes: antitumor Efficacy, Acute Toxicity, and Tissue Distribution. *Nanoscale Res Lett*. 2019;14:223. doi:10.1186/s11671-019-3057-0
57. Sun A. *Study on Construction and Pharmacokinetics of Toad Pastry Extract Long Cycle Nanoparticle Liposomes System. Master's Thesis*. Shandong University of Traditional Chinese Medicine; 2020. doi:10.27282/d.cnki.gsdzu.2019.000089
58. Wu S. *Preparation and Its Pharmacokinetic Studies in Rats of Bufadienolides Long-Circulating Liposomes. Master's Thesis*. Dalian Medical University; 2022. doi:10.26994/d.cnki.gdlyu.2016.000031

59. Li Q, Chen X, Lin W, Guo X, Ma Y. Application of a novel multicomponent nanoemulsion to tumor therapy Based on the theory of "unification of drugs and excipients". *Pharma Develop Technol*. 2023;28(3–4):351–362. doi:10.1080/10837450.2023.2196330
60. Li Y, Angelova A, Liu J, et al. In situ phase transition of microemulsions for parenteral injection yielding lyotropic liquid crystalline carriers of the antitumor drug bufalin. *Colloids Surf. B*. 2019;173:217–225. doi:10.1016/j.colsurfb.2018.09.023
61. Araceli L-V, Alejandra E-F, Alba G-F, Vicente M-C, Ramón -M-M. Biosafety of mesoporous silica nanoparticles; towards clinical translation. *Adv. Drug Delivery Rev.* 2023;201:115049. doi:10.1016/j.addr.2023.115049
62. Manzano M, Vallet-Regí M. Mesoporous Silica Nanoparticles for Drug Delivery. *Adv. Funct. Mater.* 2019;30(2):1902634. doi:10.1002/adfm.201902634
63. Khaliq NU, Lee J, Kim J, et al. Mesoporous Silica Nanoparticles as a Gene Delivery Platform for Cancer Therapy. *Pharmaceutics*. 2023;15(5):1432. doi:10.3390/pharmaceutics15051432
64. Zu M, Ma Y, Cannup B, et al. Oral delivery of natural active small molecules by polymeric nanoparticles for the treatment of inflammatory bowel diseases. *Adv. Drug Delivery Rev.* 2021;176:113887. doi:10.1016/j.addr.2021.113887
65. Zhang X, Zhang L, Liu Q, et al. Macrophage membrane-coated Eucommia ulmoides polysaccharides-loaded PLGA nanoparticles as an effective antigen-targeted delivery system. *Appl. Mater. Today*. 2024;38:102173. doi:10.1016/j.apmt.2024.102173
66. Cheng H, Zhang X, Qin L, et al. Design of self-polymerized insulin loaded poly(n-butylcyanoacrylate) nanoparticles for tunable oral delivery. *J Control Rel*. 2020;321:641–653. doi:10.1016/j.jconrel.2020.02.034
67. Sivadasan D, Ramakrishnan K, Mahendran J, et al. Solid Lipid Nanoparticles: applications and Prospects in Cancer Treatment. *Int J Mol Sci*. 2023;24(7):6199. doi:10.3390/ijms24076199
68. Pink DL, Loruthai O, Ziolek RM, Wasutrasawat P, Lorenz CDJS. On the Structure of Solid Lipid Nanoparticles. *Small*. 2019;15:1903156.
69. Kunde SS, Wairkar S. Targeted delivery of albumin nanoparticles for breast cancer: a review. *Colloids Surf. B*. 2022;213:112422. doi:10.1016/j.colsurfb.2022.112422
70. Desai N, Trieu V, Yao Z, et al. Increased antitumor activity, intratumor paclitaxel concentrations, and endothelial cell transport of cremophor-free, albumin-bound paclitaxel, ABI-007, compared with cremophor-based paclitaxel. *Clin Cancer Res*. 2006;12(4):1317–1324. doi:10.1158/1078-0432.ccr-05-1634
71. Alavi M, Webster TJ. Recent progress and challenges for polymeric microsphere compared to nanosphere drug release systems: is there a real difference? *Bioorg. Med. Chem.* 2021;33:116028. doi:10.1016/j.bmc.2021.116028
72. Rahmani F, Naderpour S, Nejad BG, et al. The recent insight in the release of anticancer drug loaded into PLGA microspheres. *Med Oncol*. 2023;40(8):229. doi:10.1007/s12032-023-02103-9
73. Yuan X, Lin S, Zhang K, Han Y. Emulsion-ultrasonic spray method to prepare polylactic acid microspheres. *Mater Lett*. 2021;309:131461. doi:10.1016/j.matlet.2021.131461
74. Li G, He Y, Han W, et al. An improved solvent evaporation method to produce poly (lactic acid) microspheres via foam-transfer. *Int J Biol Macromol*. 2021;172:114–123. doi:10.1016/j.ijbiomac.2021.01.031
75. Jin G-W, Rejinold NS, Choy J-H. Multifunctional Polymeric Micelles for Cancer Therapy. *Polymers*. 2022;14(22):4839. doi:10.3390/polym14224839
76. Atanase LI. Micellar Drug Delivery Systems Based on Natural Biopolymers. *Polymers*. 2021;13(3):477. doi:10.3390/polym13030477
77. Lin H-R, Li Y-S, Lin Y-J. Novel microencapsulated Pluronic–chitosan nanomicelles for lung delivery. *Colloid. Polym. Sci.* 2016;294(7):1209–1216. doi:10.1007/s00396-016-3879-6
78. Kotta S, Aldawsari HM, Badr-Eldin SM, Nair AB, Yt K. Progress in Polymeric Micelles for Drug Delivery Applications. *Pharmaceutics*. 2022;14(8):1636. doi:10.3390/pharmaceutics14081636
79. Wang S, Chen Y, Guo J, Huang Q. Liposomes for Tumor Targeted Therapy: a Review. *Int J Mol Sci*. 2023;24(3):2643. doi:10.3390/ijms24032643
80. Kosheli Thapa M, George Frimpong B, Xiaotong L, Zhongjian C, Wei H. Liposome-based delivery of biological drugs. *Chin. Chem. Lett.* 2021;33(2):587–596. doi:10.1016/j.cclet.2021.08.020
81. Shah S, Dhawan V, Holm R, Nagarsenker MS, Perrie Y. Liposomes: advancements and innovation in the manufacturing process. *Adv. Drug Delivery Rev.* 2020;154-155:102–122. doi:10.1016/j.addr.2020.07.002
82. Zhang M, et al. Functional nanoemulsions: controllable low-energy nanoemulsification and advanced biomedical application. *Chin. Chem. Lett.* 2023;35:108710. doi:10.1016/j.cclet.2023.108710
83. Singh M, Bharadwaj S, Lee KE, Kang SG. Therapeutic nanoemulsions in ophthalmic drug administration: concept in formulations and characterization techniques for ocular drug delivery. *J Control Rel*. 2020;328:895–916. doi:10.1016/j.jconrel.2020.10.025
84. Wu Z, Alany RG, Tawfeek N, et al. A study of microemulsions as prolonged-release injectables through in-situ phase transition. *J Control Rel*. 2014;174:188–194. doi:10.1016/j.jconrel.2013.11.022
85. Mitchell MJ, Billingsley MM, Haley RM, et al. Engineering precision nanoparticles for drug delivery. *Nat Rev Drug Discov*. 2021;20(2):101–124. doi:10.1038/s41573-020-0090-8
86. Wang J, Min J, Eghtesadi SA, Kane RS, Chilkoti A. Quantitative Study of the Interaction of Multivalent Ligand-Modified Nanoparticles with Breast Cancer Cells with Tunable Receptor Density. *ACS Nano*. 2020;14(1):372–383. doi:10.1021/acsnano.9b05689
87. Yan S, Na J, Liu X, Wu P. Different Targeting Ligands-Mediated Drug Delivery Systems for Tumor Therapy. *Pharmaceutics*. 2024;16(2):248. doi:10.3390/pharmaceutics16020248
88. Yuan Z, Yuan Y, Han L, et al. Bufalin-loaded vitamin E succinate-grafted-chitosan oligosaccharide/RGD conjugated TPGS mixed micelles demonstrated improved antitumor activity against drug-resistant colon cancer. *Int j Nanomed*. 2018;13:7533–7548. doi:10.2147/ijn.S170692
89. Lan X, Shuli M, Bozhen F, Zeting Y, Peihao Y. Bufalin-loaded vitamin E succinate-grafted chitosan oligosaccharide/RGD-conjugated TPGS mixed micelles inhibit intraperitoneal metastasis of ovarian cancer. *Cancer Nanotechnol.* 2023;25. doi:10.1186/s12645-023-00178-7
90. Feng S. *Study on Bufalin Loaded Vec/T Mixed Micelle Decorated with RGD. Master's Thesis*. East China University of Science and Technology; 2021. doi:10.27148/d.cnki.ghagu.2017.000035
91. Yin P, Wang Y, Qiu Y, et al. Bufalin-loaded mPEG-PLGA-PLL-cRGD nanoparticles: preparation, cellular uptake, tissue distribution, and anticancer activity. *Int j Nanomed*. 2012;7:3961–3969. doi:10.2147/ijn.S32063

92. Zhang Y, Tian Z, Zhao X, et al. Dual-modified Bufalin loaded liposomes for enhanced tumor targeting. *Colloids Surf. A*. 2019;571:72–79. doi:10.1016/j.colsurfa.2019.03.060
93. Dong H, Tian L, Gao M, et al. Promising galactose-decorated biodegradable poloxamer 188-PLGA diblock copolymer nanoparticles of resibufogenin for enhancing liver cancer therapy. *Drug Delivery*. 2017;24(1):1302–1316. doi:10.1080/10717544.2017.1373165
94. W. L, et al. Preparation and evaluation of bufogenin lipid-protein hybrid nanoparticles. *Chin J Pharm*. 2016;14:160–174. doi:10.14146/j.cnki.cjp.2016.05.003
95. Xu Y, Tang L, Chen P, et al. Tumor-Targeted Delivery of Bufalin-Loaded Modified Albumin-Polymer Hybrid for Enhanced Antitumor Therapy and Attenuated Hemolysis Toxicity and Cardiotoxicity. *AAPS Pharm Sci Tech*. 2021;22(4):137. doi:10.1208/s12249-021-02000-2
96. Xu Y, Liu Y, Liu Q, et al. Co-delivery of bufalin and nintedanib via albumin sub-microspheres for synergistic cancer therapy. *J Control Rel*. 2021;338:705–718. doi:10.1016/j.jconrel.2021.08.049
97. Liu Y, Lu X, Zhang Z, Jiang S, Lv H. mPEG-Cholic acid/TPGS mixed micelles for combined delivery of paclitaxel and bufalin to treat hepatocellular carcinoma. *Pharma Develop Technol*. 2022;27(2):215–227. doi:10.1080/10837450.2022.2037140
98. Guo B, et al. Preparation of folate receptor targeted long-circulating liposomes loaded venenum bufonis extract and in vitro anti-tumor activity evaluation. *J Guangdong Pharm Univ*. 2017;33:569–574. doi:10.16809/j.cnki.2096-3653.2017052801
99. Zou A, Zhao X, Handge UA, et al. Folate receptor targeted bufalin/β-cyclodextrin supramolecular inclusion complex for enhanced solubility and anti-tumor efficiency of bufalin. *Mater Sci Eng C Mater Biol Appl*. 2017;78:609–618. doi:10.1016/j.msec.2017.04.094
100. Luo H, et al. Preparation and evaluation in vitro of folic acid-modified bufalin cationic liposomes. *J Hunan Univ Chin Med*. 2023;43:822–829. doi:10.3969/j.issn.1674-070X.2023.05.010
101. Ning Z, Zhao Y, Yan X, Hua Y, Meng Z. Flower-like Composite Material Delivery of Co-Packaged Lenvatinib and Bufalin Prevents the Migration and Invasion of Cholangiocarcinoma. *Nanomaterials*. 2022;12(12):2048. doi:10.3390/nano12122048
102. Chen Q, Liu J. Transferrin and folic acid co-modified bufalin-loaded nanoliposomes: preparation, characterization, and application in anticancer activity. *Int j Nanomed*. 2018;13:6009–6018. doi:10.2147/ijn.s176012
103. Xu J, Sun Y, Yuan Z, et al. Bufalin-Loaded CaP/DPPE-PEG-EGF Nanospheres: preparation, Cellular Uptake, Distribution, and Anti-Tumor Effects. *J Biomed Nanotechnol*. 2019;15(2):329–339. doi:10.1166/jbn.2019.2681
104. Huang N. *Construction of Compound Immunoliposomes Loaded with Melittin and Bufalin and Its Synergistic Mechanism in Inhibiting Sorafenib Resistance in Hepatocellular Carinoma. PhD Thesis*. Naval Medical University; 2019.
105. Tian X, Yin H, Zhang S, et al. Bufalin loaded biotinylated chitosan nanoparticles: an efficient drug delivery system for targeted chemotherapy against breast carcinoma. *Euro J Pharm Biopharm*. 2014;87(3):445–453. doi:10.1016/j.ejpb.2014.05.010
106. Li Y, Yuan J, Yang Q, et al. Immunoliposome co-delivery of bufalin and anti-CD40 antibody adjuvant induces synergetic therapeutic efficacy against melanoma. *Int j Nanomed*. 2014;9:5683–5700. doi:10.2147/ijn.S73651
107. Haake SM, Rios BL, Pozzi A, Zent R. Integrating integrins with the hallmarks of cancer. *Mat Biol*. 2024;130:20–35. doi:10.1016/j.matbio.2024.04.003
108. Hua Y, Yu C. Research progress on asialoglycoprotein receptor-targeted radiotracers designed for hepatic nuclear medicine imaging. *Eur. J. Med. Chem.* 2024;269:116278. doi:10.1016/j.ejmech.2024.116278
109. Anter HM, Aman RM, Othman DIA, et al. Apocynin-loaded PLGA nanomedicine tailored with galactosylated chitosan intrigue asialoglycoprotein receptor in hepatic carcinoma: prospective targeted therapy. *Int J Pharm*. 2023;631:122536. doi:10.1016/j.ijpharm.2022.122536
110. Zhang X, Huang G. Synthetic lipoprotein as nano-material vehicle in the targeted drug delivery. *Drug Delivery*. 2017;24(2):16–21. doi:10.1080/10717544.2017.1384518
111. Wu L, Feng J, Li J, et al. The gut microbiome-bile acid axis in hepatocarcinogenesis. *Biomed. Pharmacother.* 2021;133:111036. doi:10.1016/j.biopha.2020.111036
112. Shmendel EV, Puchkov PA, Maslov MA. Design of Folate-Containing Liposomal Nucleic Acid Delivery Systems for Antitumor Therapy. *Pharmaceutics*. 2023;15(5):1400. doi:10.3390/pharmaceutics15051400
113. Mi X, Hu M, Dong M, et al. Folic Acid Decorated Zeolitic Imidazolate Framework (ZIF-8) Loaded with Baicalin as a Nano-Drug Delivery System for Breast Cancer Therapy. *Int j Nanomed*. 2021;16:8337–8352. doi:10.2147/ijn.S340764
114. Zhao X, Yang Y, Su X, et al. Transferrin-Modified Triptolide Liposome Targeting Enhances Anti-Hepatocellular Carcinoma Effects. *Biomedicines*. 2023;11(10):2869. doi:10.3390/biomedicines11102869
115. Moreira TDS, Silva ADO, Vasconcelos BRF, et al. DOPE/CHEMS-Based EGFR-Targeted Immunoliposomes for Docetaxel Delivery: formulation Development, Physicochemical Characterization and Biological Evaluation on Prostate Cancer Cells. *Pharmaceutics*. 2023;15(3):0915. doi:10.3390/pharmaceutics15030915
116. Tripathi R, Guglani A, Ghorpade R, Wang B. Biotin conjugates in targeted drug delivery: is it mediated by a biotin transporter, a yet to be identified receptor, or (an)other unknown mechanism(s)? *J Enz Inhib Med Chem*. 2023;38(1):2276663. doi:10.1080/14756366.2023.2276663
117. Singh A, Ranjan A. Adrenergic receptor signaling regulates the CD40-receptor mediated anti-tumor immunity. *Front Immunol*. 2023;14:1141712. doi:10.3389/fimmu.2023.1141712
118. Krishnan N, Fang RH, Zhang L. Cell membrane-coated nanoparticles for the treatment of cancer. *Clinical and Translational Medicine*. 2023;13(6):e1285. doi:10.1002/ctm2.1285
119. Paloma P, Aravind Kumar R. Cancer Cell Membrane Cloaked Nanocarriers: a Biomimetic Approach Towards Cancer Theranostics. *Mater Today Commun*. 2022;33:104289. doi:10.1016/j.mtcomm.2022.104289
120. Wang H, Bremner DH, Wu K, et al. Platelet membrane biomimetic bufalin-loaded hollow MnO2 nanoparticles for MRI-guided chemo-chemodynamic combined therapy of cancer. *Chem Eng J*. 2019;382:122848. doi:10.1016/j.cej.2019.122848
121. Wang H, Wu J, Williams GR, et al. Platelet-membrane-biomimetic nanoparticles for targeted antitumor drug delivery. *J Nanobiotechnol*. 2019;17(1):60. doi:10.1186/s12951-019-0494-y
122. Fan J, Liu B, Long Y, et al. Sequentially-targeted biomimetic nano drug system for triple-negative breast cancer ablation and lung metastasis inhibition. *Acta Biomater.* 2020;113:554–569. doi:10.1016/j.actbio.2020.06.025
123. Liu B, Wang W, Fan J, et al. RBC membrane camouflaged Prussian blue nanoparticles for gamabutolin loading and combined chemo/photothermal therapy of breast cancer. *Biomaterials*. 2019;217:119301. doi:10.1016/j.biomaterials.2019.119301

124. Zhang W, Fan Y, Zhang J, et al. Cell membrane-camouflaged bufalin targets NOD2 and overcomes multidrug resistance in pancreatic cancer. *Drug Resist Updates*. 2023;71:101005. doi:10.1016/j.drup.2023.101005
125. Zibin S, Zhao L, Fang W, et al. Glioma cell membrane camouflaged cinobufotalin delivery system for combinatorial orthotopic glioblastoma therapy. *Nano Res*. 2023;16(8):11164–11175. doi:10.1007/s12274-023-5807-7
126. Long Y, Wang Z, Fan J, et al. A hybrid membrane coating nanodrug system against gastric cancer via the VEGFR2/STAT3 signaling pathway. *J Mat Chem B*. 2021;9(18):3838–3855. doi:10.1039/d1tb00029b
127. Luo M, Tan C, Cao R, et al. Hybrid membrane camouflaged Prussian blue nanoparticles with cinobufagin loading for chemo/photothermal therapy of colorectal cancer. *Mater Des*. 2023;232:112088. doi:10.1016/j.matdes.2023.112088
128. Zeng Z, Wang Z, Chen S, et al. Bio-nanocomplexes with autonomous O2 generation efficiently inhibit triple negative breast cancer through enhanced chemo-PDT. *J Nanobiotechnol*. 2022;20(1):500. doi:10.1186/s12951-022-01706-0
129. Long Y, Fan J, Zhou N, et al. Biomimetic Prussian blue nanocomplexes for chemo-photothermal treatment of triple-negative breast cancer by enhancing ICD. *Biomaterials*. 2023;303:122369. doi:10.1016/j.biomaterials.2023.122369
130. Fan J, Qin Y, Xiao C, et al. Biomimetic PLGA-based nanocomplexes for improved tumor penetration to enhance chemo-photodynamic therapy against metastasis of TNBC. *Mater Today Adv*. 2022;16:100289. doi:10.1016/j.mtadv.2022.100289
131. Xiao C, Tong C, Fan J, et al. Biomimetic nanoparticles loading with gamabutolin-indomethacin for chemo/photothermal therapy of cervical cancer and anti-inflammation. *J Control Rel*. 2021;339:259–273. doi:10.1016/j.jconrel.2021.09.034
132. Han H, Bártolo R, Li J, Shahbazi MA, Santos HA. Biomimetic platelet membrane-coated nanoparticles for targeted therapy. *Euro J Pharm Biopharm*. 2022;172:1–15. doi:10.1016/j.ejpb.2022.01.004
133. Nguyen PHD, Jayasinghe MK, Le AH, Peng B, Le MTN. Advances in Drug Delivery Systems Based on Red Blood Cells and Their Membrane-Derived Nanoparticles. *ACS Nano*. 2023;17(6):5187–5210. doi:10.1021/acsnano.2c11965
134. Li Y, Ke J, Jia H, et al. Cancer cell membrane coated PLGA nanoparticles as biomimetic drug delivery system for improved cancer therapy. *Colloids Surf B*. 2023;222:113131. doi:10.1016/j.colsurfb.2023.113131
135. Cheng R, Wang S. Cell-mediated nanoparticle delivery systems: towards precision nanomedicine. *Drug Delivery Transl Res*. 2024. doi:10.1007/s13346-024-01591-0
136. Liang J, Yang B, Zhou X, et al. Stimuli-responsive drug delivery systems for head and neck cancer therapy. *Drug Delivery*. 2021;28(1):272–284. doi:10.1080/10717544.2021.1876182
137. Gheysoori P, Paydayesh A, Jafari M, Peidayesh HJEPJ. Thermoresponsive nanocomposite hydrogels based on Gelatin/poly (N–isopropylacrylamide) (PNIPAM) for controlled drug delivery. *Eur Polymer J*. 2023;186:111846.
138. Murugan B, Sagadevan S, Fatimah I, et al. Smart stimuli-responsive nanocarriers for the cancer therapy – nanomedicine. *Nanotechnol Rev*. 2021;10(1):933–953. doi:10.1515/ntrev-2021-0067
139. Wang Y, Deng T, Liu X, et al. Smart Nanoplatforms Responding to the Tumor Microenvironment for Precise Drug Delivery in Cancer Therapy. *Int j Nanomed*. 2024;19:6253–6277. doi:10.2147/ijn.s459710
140. Gou H, Huang RC, Zhang FL, Su YH. Design of dual targeting immunomicelles loaded with bufalin and study of their anti-tumor effect on liver cancer. *J Integr Med*. 2021;19(5):408–417. doi:10.1016/j.joim.2021.05.001
141. Yue Y, Li H, Wang X, et al. Intelligent Responsive Nanoparticles with Multilevel Triggered Drug Penetration for Tumor Photochemotherapy. *ACS Appl. Mater. Interfaces*. 2023;15(37):44175–44185. doi:10.1021/acsami.3c06674
142. He J, Chen G, Zhao P, Ou C. Near-infrared light-controllable bufalin delivery from a black phosphorus-hybrid supramolecular hydrogel for synergistic photothermal-chemo tumor therapy. *Nano Res*. 2021;14(11):3988–3998. doi:10.1007/s12274-021-3325-z
143. Zhang X, Ma Y, Shi Y, et al. Advances in liposomes loaded with Photoresponse materials for cancer therapy. *Biomed Pharmacothe*. 2024;174:116586. doi:10.1016/j.biopha.2024.116586
144. Yuan Z, Liu C, Sun Y, et al. Bufalin exacerbates Photodynamic therapy of colorectal cancer by targeting SRC-3/HIF-1α pathway. *Int J Pharm*. 2022;624:122018. doi:10.1016/j.ijpharm.2022.122018
145. Bulatao BP, Nalinratana N, Jantaratana P, et al. Lutein-loaded chitosan/alginate-coated Fe(3)O(4) nanoparticles as effective targeted carriers for breast cancer treatment. *Int J Biol Macromol*. 2023;242:124673. doi:10.1016/j.ijbiomac.2023.124673
146. Hu W. *Preliminary Study on Anti-Metastasis of Breast Cancer by Photomagnetic Dual-Sensitive Bufalin Liposomes. Master's Thesis*. Beijing University of Chinese Medicine; 2022. doi:10.26973/d.cnki.gbjzu.2022.000197
147. Li R, Peng F, Cai J, Yang D, Zhang P. Redox dual-stimuli responsive drug delivery systems for improving tumor-targeting ability and reducing adverse side effects. *Asian J. Pharm. Sci.* 2020;15(3):311–325. doi:10.1016/j.ajps.2019.06.003
148. Wang H, Williams GR, Wu J, et al. Pluronic F127-based micelles for tumor-targeted bufalin delivery. *Int J Pharm*. 2019;559:289–298. doi:10.1016/j.ijpharm.2019.01.049
149. Feng Q, Bennett Z, Grichuk A, et al. Severely polarized extracellular acidity around tumour cells. *Nat Biomed Eng*. 2024. doi:10.1038/s41551-024-01178-7
150. Chen B, Zhao Y, Lin Z, et al. Apatinib and gamabufotalin co-loaded lipid/Prussian blue nanoparticles for synergistic therapy to gastric cancer with metastasis. *J Pharm Anal*. 2024;14(5):100904. doi:10.1016/j.jpha.2023.11.011
151. Zeng H, Xia C, Zhao B, et al. Folic Acid-Functionalized Metal-Organic Framework Nanoparticles as Drug Carriers Improved Bufalin Antitumor Activity Against Breast Cancer. *Front Pharmacol*. 2021;12:747992. doi:10.3389/fphar.2021.747992
152. Li J, Zhang Z, Deng H, Zheng Z. Cinobufagin-Loaded and Folic Acid-Modified Polydopamine Nanomedicine Combined With Photothermal Therapy for the Treatment of Lung Cancer. *Front Chem*. 2021;9:637754. doi:10.3389/fchem.2021.637754
153. Ruxia L, et al. Identification of anti-tumor constituents from toad skin and toad venom by UPLC-QTOF/MS in-depth chemical profiling combined with bioactivity-based molecular networking. *Arabian J. Chem.* 2023;17:105427. doi:10.1016/j.arabjc.2023.105427
154. Cheng CS, Wang J, Chen J, et al. New therapeutic aspects of steroidal cardiac glycosides: the anticancer properties of Huachansu and its main active constituent Bufalin. *Can Cell Inter*. 2019;19(1):92. doi:10.1186/s12935-019-0806-1
155. Yang L, Zhou F, Zhuang Y, et al. Acetyl-bufalin shows potent efficacy against non-small-cell lung cancer by targeting the CDK9/STAT3 signalling pathway. *Br. J. Cancer*. 2021;124(3):645–657. doi:10.1038/s41416-020-01135-6
156. Soni A, Bhandari MP, Tripathi GK, et al. Nano-biotechnology in tumour and cancerous disease: a perspective review. *J Cell & Mol Med*. 2023;27(6):737–762. doi:10.1111/jcmm.17677

157. Tian H, Zhao F, Qi Q, Yue B, Zhai B. Targeted drug delivery systems for elemene in cancer therapy: the story thus far. *Biomed. Pharmacother.* 2023;166:115331. doi:10.1016/j.biopha.2023.115331
158. Sun Q, Ojha T, Kiessling F, Lammers T, Shi Y. Enhancing Tumor Penetration of Nanomedicines. *Biomacromolecules*. 2017;18(5):1449–1459. doi:10.1021/acs.biomac.7b00068
159. Sharanya K, Pravin Kumar S, Gun Anit K, Ashutosh T. Trends in smart drug delivery systems for targeting cancer cells. *Materials Science and Engineering: B*. 2023;297:116816. doi:10.1016/j.mseb.2023.116816
160. Arranja AG, Pathak V, Lammers T, Shi Y. Tumor-targeted nanomedicines for cancer theranostics. *Pharmacol Res*. 2017;115:87–95. doi:10.1016/j.phrs.2016.11.014
161. Sun R, Dai J, Ling M, et al. Delivery of triptolide: a combination of traditional Chinese medicine and nanomedicine. *J Nanobiotechnol*. 2022;20(1):194. doi:10.1186/s12951-022-01389-7
162. Martínez-Negro M, González-Rubio G, Aicart E, et al. Insights into colloidal nanoparticle-protein Corona interactions for nanomedicine applications. *Adv. Colloid Interface Sci.* 2021;289:102366. doi:10.1016/j.cis.2021.102366
163. Dexin Z, et al. Biomedical Applications of Cell Membrane-Based Biomimetic Nano-Delivery System. *Adv Ther*. 2023;6. doi:10.1002/adtp.202300304
164. Chang M, Dong C, Huang H, et al. Nanobiomimetic Medicine. *Adv. Funct. Mater.* 2022;32(32):2204791. doi:10.1002/adfm.202204791
165. Zhang Q, Kuang G, Li W, et al. Stimuli-Responsive Gene Delivery Nanocarriers for Cancer Therapy. *Nano-Micro Lett*. 2023;15(1):44. doi:10.1007/s40820-023-01018-4
166. Fatima M, Almalki WH, Khan T, Sahebkar A, Kesharwani P. *Harnessing the Power of Stimuli-Responsive Nanoparticles as an Effective Therapeutic Drug Delivery System*. *Adv. Mater.* 2024;e2312939. doi:10.1002/adma.202312939
167. Xiang Z, Liu M, Song J. Stimuli-Responsive Polymeric Nanosystems for Controlled Drug Delivery. *Appl Sci*. 2021;11(20):9541. doi:10.3390/app11209541
168. Zou J, Li M, Liu Z, et al. Unleashing the potential: integrating nano-delivery systems with traditional Chinese medicine. *Nanoscale*. 2024;16(18):8791–8806. doi:10.1039/d3nr06102g
169. Almalki WH. Challenging paradigms in tumour drug delivery. *Nature Mater.* 2020;19(5):477. doi:10.1038/s41563-020-0676-x
170. Cheng YH, He C, Riviere JE, Monteiro-Riviere NA, Lin Z. Meta-Analysis of Nanoparticle Delivery to Tumors Using a Physiologically Based Pharmacokinetic Modeling and Simulation Approach. *ACS Nano*. 2020;14(3):3075–3095. doi:10.1021/acsnano.9b08142
171. Ji T, Kohane DS. Nanoscale systems for local drug delivery. *Nano Today.* 2019;28:100765. doi:10.1016/j.nantod.2019.100765
172. Dosta P, Dion MZ, Prado M, et al. Matrix Metalloproteinase- and pH-Sensitive Nanoparticle System Enhances Drug Retention and Penetration in Glioblastoma. *ACS Nano*. 2024;18(22):14145–14160. doi:10.1021/acsnano.3c03409
173. Mohammadi M, Karimi M, Malaekeh-Nikouei B, Torkashvand M, Alibolandi M. Hybrid in situ- forming injectable hydrogels for local cancer therapy. *Int J Pharm*. 2022;616:121534. doi:10.1016/j.ijpharm.2022.121534
174. Yuniarsih N, Chaerunisaa AY, Elamin KM, Wathoni N. Polymeric Nanohydrogel in Topical Drug Delivery System. *Int j Nanomed*. 2024;19:2733–2754. doi:10.2147/ijn.S442123
175. Bobo D, Robinson KJ, Islam J, Thurecht KJ, Corrie SR. Nanoparticle-Based Medicines: a Review of FDA-Approved Materials and Clinical Trials to Date. *Pharm Res*. 2016;33(10):2373–2387. doi:10.1007/s11095-016-1958-5
176. Fan D, Cao Y, Cao M, et al. Nanomedicine in cancer therapy. *Sig Transd Tar Ther*. 2023;8(1):293. doi:10.1038/s41392-023-01536-y
177. Younis MA, Tawfeek HM, Abdellatif AAH, Abdel-Aleem JA, Harashima H. Clinical translation of nanomedicines: challenges, opportunities, and keys. *Adv Drug Deliv Rev.* 2022;181:114083. doi:10.1016/j.addr.2021.114083